Call for Bids NS15-1 – Exploration history, geologic setting, and exploration potential: *Western and Central regions*

Mark E. Deptuck*, David E. Brown, and Brian Altheim

Canada-Nova Scotia Offshore Petroleum Board, Halifax, Nova Scotia, Canada

* mdeptuck@cnsopb.ns.ca

1. Overview

The NS15-1 Call for Bids includes nine parcels that are clustered into three geographically and geologically distinct areas (Figure 1.1). Parcels 1, 2, 3, and 4 are located on the outer shelf and slope along the southwestern most parts of the Scotian margin, adjacent to and seaward of Georges Bank (Western Region). Parcels 5, 6, and 7 are located on the outer shelf and upper slope of the central Scotian margin, west of the Sable Island and the Sable Subbasin (Central Region). Parcels 8 and 9 are located above existing oil and gas discoveries on the shelf in the Sable Subbasin, north and east of Sable Island – these being the Penobscot oil discovery in fluvial-deltaic sandstones of the Missisauga Formation and the Eagle discovery in chalks of the Wyandot Formation (Figure 1.2), respectively (Eastern Region). This document describes the exploration history, geologic setting, and exploration potential for the ***Western*** and ***Central*** regions.

2. Western Region

Exploration history

The southwestern Scotian margin, stretching from Georges Bank across the Northeast Channel, and to the LaHave Bank (Figures 1.1, 2.1) is the most lightly explored area of the Scotian Basin. Limited coverage of modern seismic data-sets, especially on the shelf, coupled with very sparse well control, also makes this one of the most poorly understood offshore regions of Nova Scotia. Only four wells provide stratigraphic calibration in an area covering more than 28 000 km^2. With Montagnais I-94 (Parcel 4) penetrating the central uplift of an Eocene impact crater (see Deptuck and Campbell, 2012), only Mohawk B-93 (Parcel 4; drilled in 1970) and Bonnet P-23 (Parcel 3; drilled in 1984) provide calibration for Mesozoic strata on the southwestern Scotian Shelf. A fourth well, Shelburne G-29 (drilled in 1985) provides the only stratigraphic calibration of the southwestern Scotian Slope. It lies along the easternmost edge of study area, more than 30 km east of Parcel 4, and provides little calibration of pre-Cretaceous strata. Additional calibration is available roughly 250 km southwest of Bonnet on the U.S. side of Georges Bank, where ten wells were drilled on the shelf in the 1970's and early 80's (Figure 2.1).

Exploration started on the southwestern part of the margin in the late 1960s with the acquisition of regional seismic and gravity-magnetic data on the Scotian Shelf / LaHave Platform, followed by two wells in the early 1970s. Exploration along the Abenaki carbonate reef complex and along the upper Scotian Slope resulted in two additional wells in the 1980s. Large basin-scale regional seismic programs were completed in the late 1990s with emphasis on the deep water slope, and while the deep water slope was licensed by industry and some additional seismic acquired, no wells were drilled. Figure 2.2 shows the distribution of seismic data acquired since 1970, and the location of wells.

The first well in the western region was Shell **Mohawk B-93** (1970) and was also the fifth drilled in the Scotian Basin. It is located in 117 m water and was designed to test a drape feature above a basement horst block inboard of the basin hingeline fault (Figures 2.3, 2.4). Four-way simple closure was mapped at the top of the Late Jurassic Abenaki Formation and reservoirs were

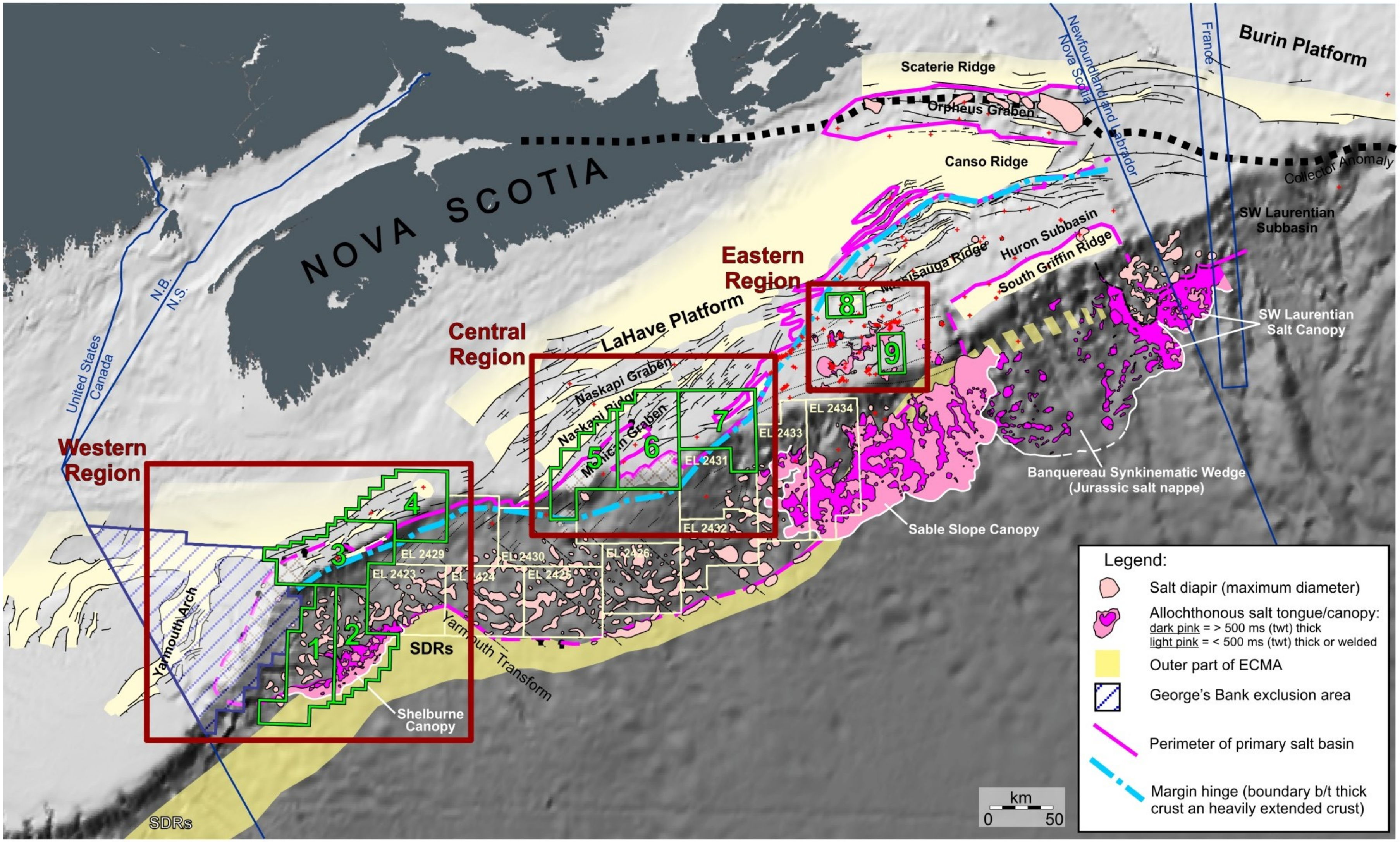

Figure 1.1 Basemap of the Scotian margin showing distribution of key structural elements. Some faults north of the Naskapi Ridge are from Wade and MacLean (1990). Most other elements are from Deptuck and Kendell (in prep).

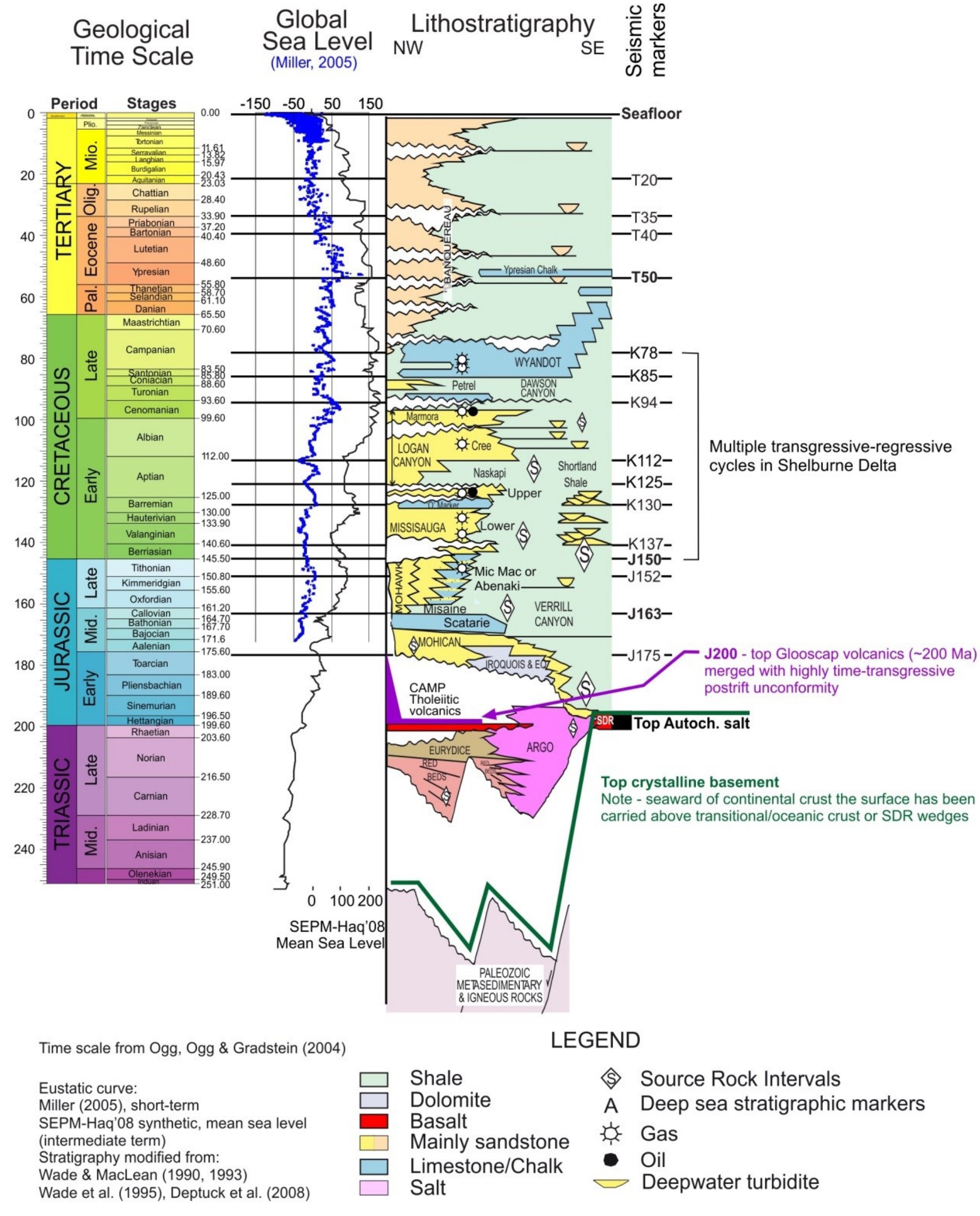

Figure 1.2 Stratigraphic column adpated from OETR (2011), with key seismic markers.

expected within the Abenaki and underlying (then unnamed) fluvial siliciclastics. Some minor porosity was present in Abenaki oolitic limestones though the dominant underlying coarse-grained fluvial sandstones (Mohican Formation type section) had good to excellent porosity but no oil or gas shows. The well bottomed in Middle Devonian granitic basement at a total depth of 2124 m.

Another large basement feature was tested by the Union **Montagnais I-94** well in 1974 (Figures 2.3, 2.4). 2D seismic data defined a drape feature with presumed simple four-way closure on an isolated basement high at the edge of the basin hingeline fault. The high was surrounded by a depression and a complexly faulted outer margin. The well was spudded in 113 m water depth and penetrated a thin clay-dominated Tertiary section followed by Early Cretaceous Logan Canyon Formation fluvial sandstones and shales. Well TD was at 1644 m in highly deformed Cambro-Ordovician metaquartzites of the Meguma Supergroup. Subsequent petrographic study of the basement core and the feature's structural architecture revealed it was an impact crater with an event age of ~50.5 Ma (Early Eocene). A shallow minor gas show was found at 377.6-383.7 m in unconsolidated Quaternary gravels but was not tested.

The Petro-Canada **Bonnet P-23** well (1984) is the westernmost well in the Scotian Basin. It was drilled to test a large (~70 km^2), elongate, fault-bounded structure located about 6 km inboard of the highly faulted bank margin in 133.5 m water. Closure was mapped at the interpreted Late Jurassic Mohawk seismic horizon, with its fluvial sandstones the primary reservoir target. About 1700 m of Tertiary mudstones are above several base Tertiary unconformities that cut down through the Cretaceous section leaving a thin (~25 m) interval of Late Cretaceous sandstones and shales. This was followed by the entire Middle to Late Jurassic Abenaki Formation (Roseway-Baccaro-Misaine-Scatarie members; Figure 1.2). The carbonates are dominately oolitic limestones and minor dolomites having occasional fair (inter-oolitic), to very good (intercrystalline dolomitic) porosity in lagoonal facies mudstones. No reef-related facies were present. Rare porosity was found in the thick underlying Early Jurassic Iroquois Formation dolomites though the basal 450 m of this formation was not accurately evaluated due to extensive lost circulation zones, incomplete mud-gas logging, lost mud and sample returns, etc. that may be the result of enhanced porous intervals or the presence of several large faults in this section. Four gas peaks under 100 TGU were encountered here and minor oil staining in two samples but no tests done. Expected coeval Mohawk or Mohican sandstones were not present and the well TD was at 4336 m in the Iroquois Formation.

The fourth well, **Shelburne G-29** was drilled by Petro-Canada in 1985 and is outside of the Call parcels, 30 km east of Parcel 4. It was spudded in 1153.5 m water with the primary target an interpreted turbidite fan of Paleocene to possibly Maastrichtian age. The secondary target was an underlying southwest-plunging structural nose of the Jurassic Abenaki carbonate margin (Middle Jurassic Scatarie Member) and dolomitic Iroquois Formation above a salt pillow. A few minor sandstones with scattered fair to very good porosity were encountered in the upper Tertiary. In the target interval (later confirmed to be the Late Cretaceous Wyandot and Dawson Canyon formations), the suspected turbidite fan was found to be a succession of limestones, marls and shales, with the remaining interval being almost entirely shale. The well just tagged the top of the Abenaki Formation (Baccaro Member) and a core was attempted. However, after cutting 14.5 m of core the drill string became stuck while pulling out of the hole and following unsuccessful attempts to retrieve it the well was abandoned at a TD of 4005.5 m. No reservoirs or hydrocarbon shows were present.

Geological Setting

Parcels 1, 2, 3, and 4 in the NS15-1 Call for Bids are located on the outer shelf and slope of the southwestern most Scotian margin, east of the Georges Bank moratorium area and existing (but inactive) BP and Chevron exploration permits, and west of Shell's Exploration Licences 2423 and 2429 (Figures 1.1, 2.1). The parcels sit above the westernmost parts of the

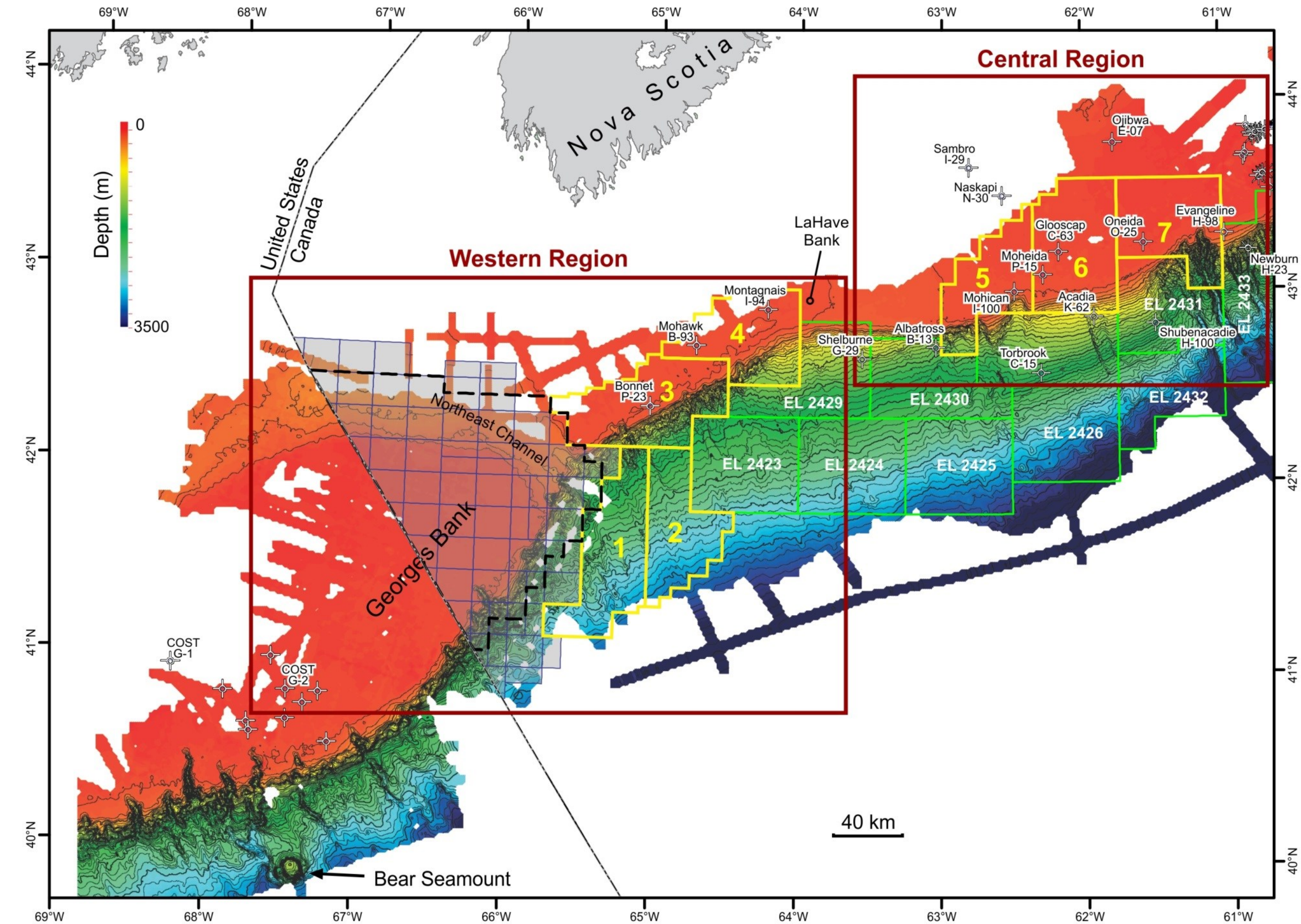

Figure 2.1 Depth map of the modern seafloor, gridded from available seismic programs off southern and central Nova Scotia. Yellow polygons correspond to the seven western parcels in the NS15-1 Call for Bids. Green polygons identify exploration licences held by Shell and BP. Grey boxes identify exploration permits held by Chevron and BP in the area of the Georges Bank Moratorium (black hachure line).

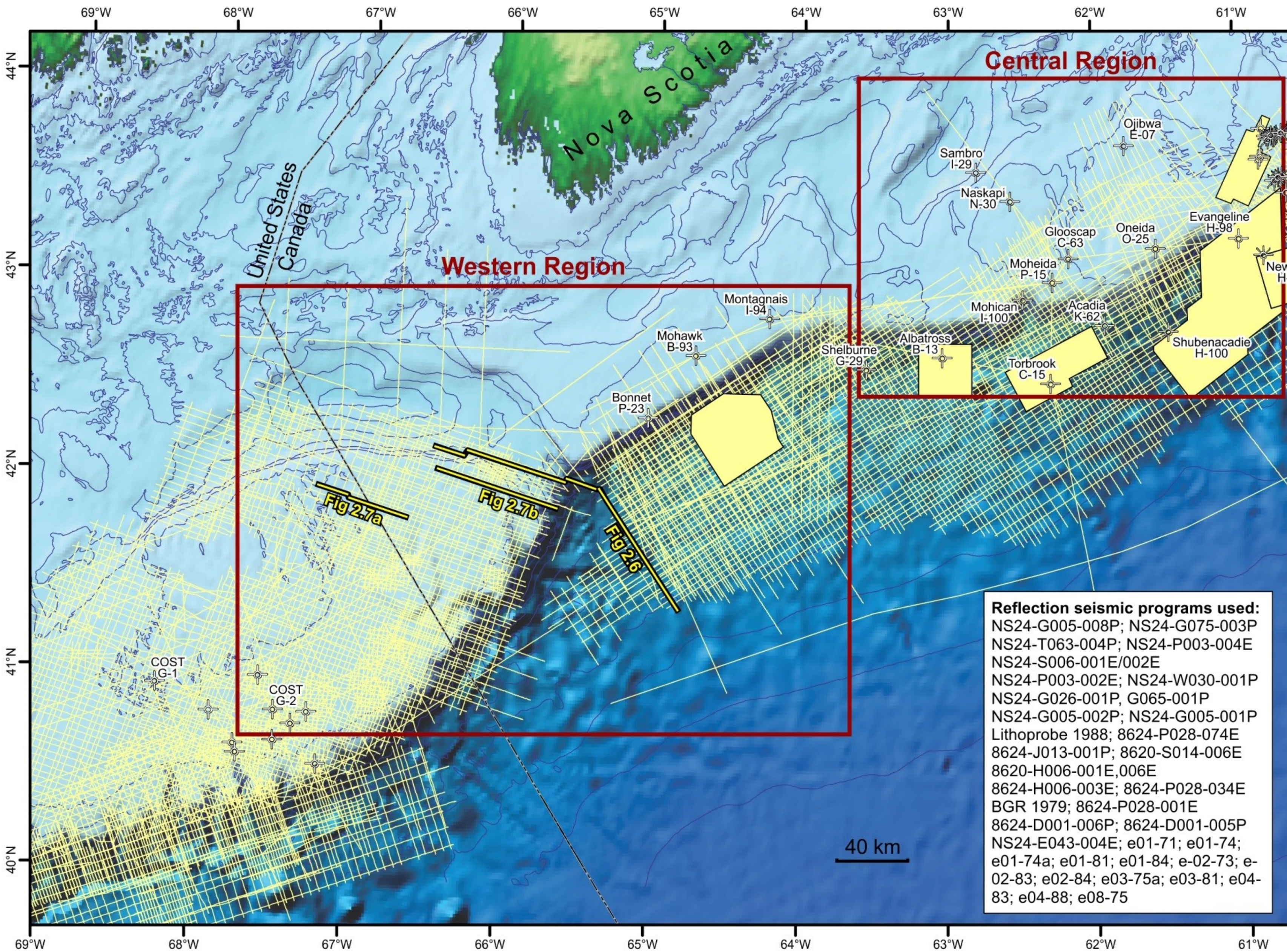

Figure 2.2. Seafloor bathymetry (NOAA ETOPO1) overlain by digital seismic data-set. Seismic program numbers listed in the inset.

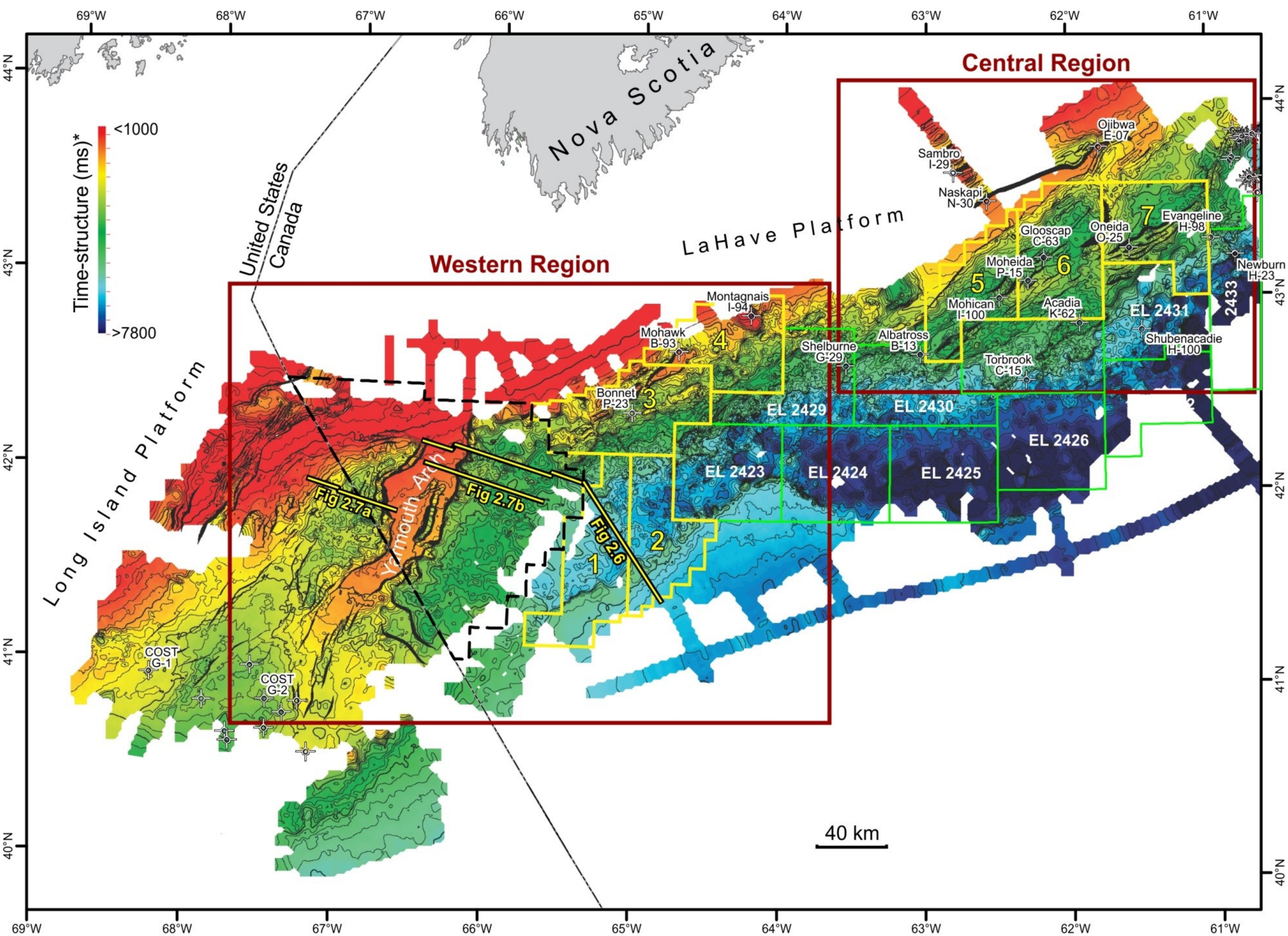

Figure 2.3 Time-structure map of the top of crystalline basement. In deepwater this surface was carried above oceanic or transitional crust (or above seaward dipping reflections where present). As such, the surface is highly diachronous. In some areas, particularly on the slope, the surface is approximate and has almost certainly been carried too shallow. *Note that the water column was depth converted, removing the associated velocity sag caused by increasing water depths.

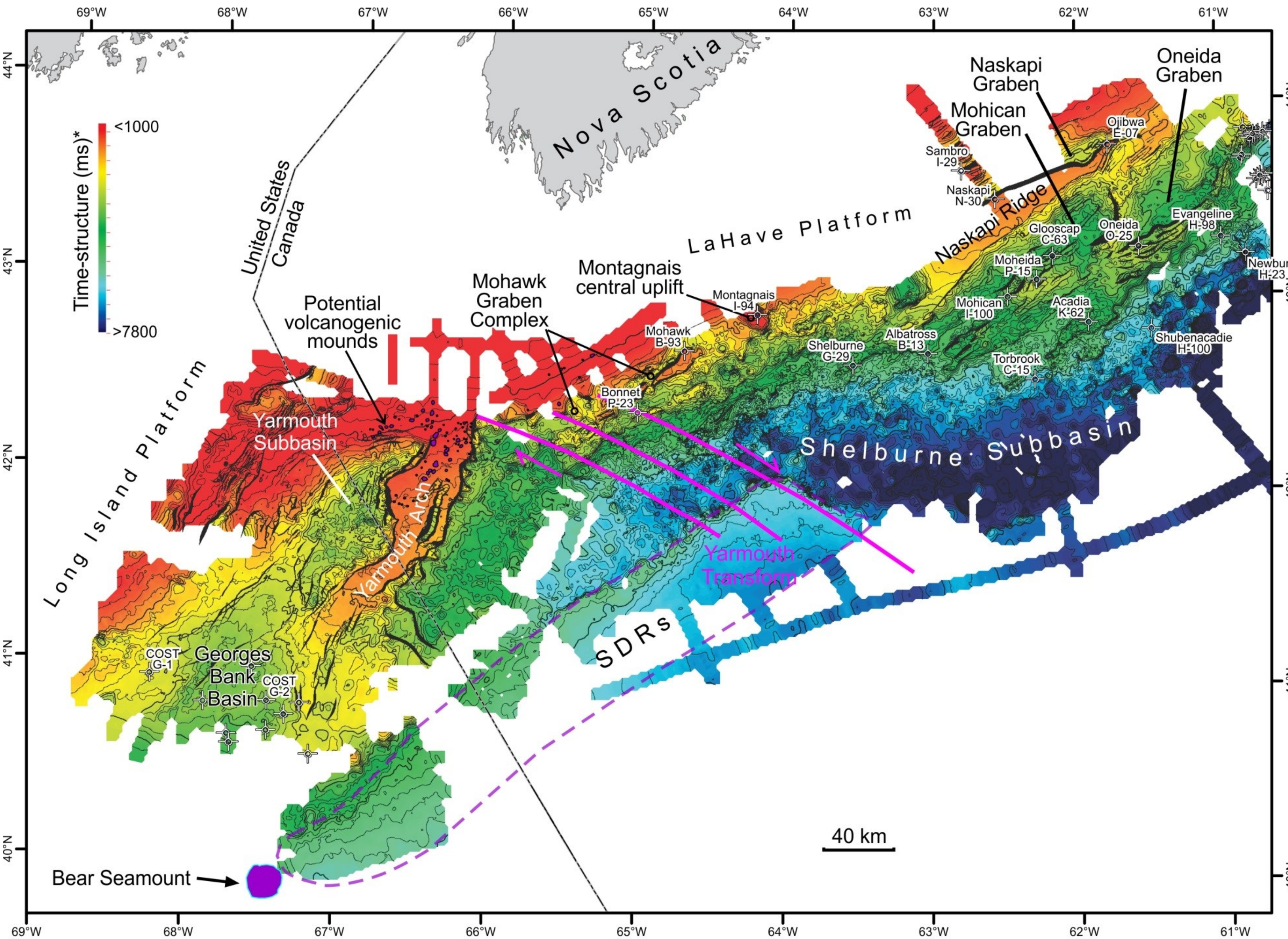

Figure 2.4 Time-structure map of the top of crystalline basement with some annotation removed. In deepwater this surface was carried above oceanic or transitional crust (or above seaward dipping reflections where present). As such, the surface is highly diachronous. In some areas, particularly on the slope, the surface is approximate and has almost certainly been carried too shallow. *Note that the water column was depth converted, removing the associated velocity sag caused by increasing water depths.

Deptuck et al. 2015

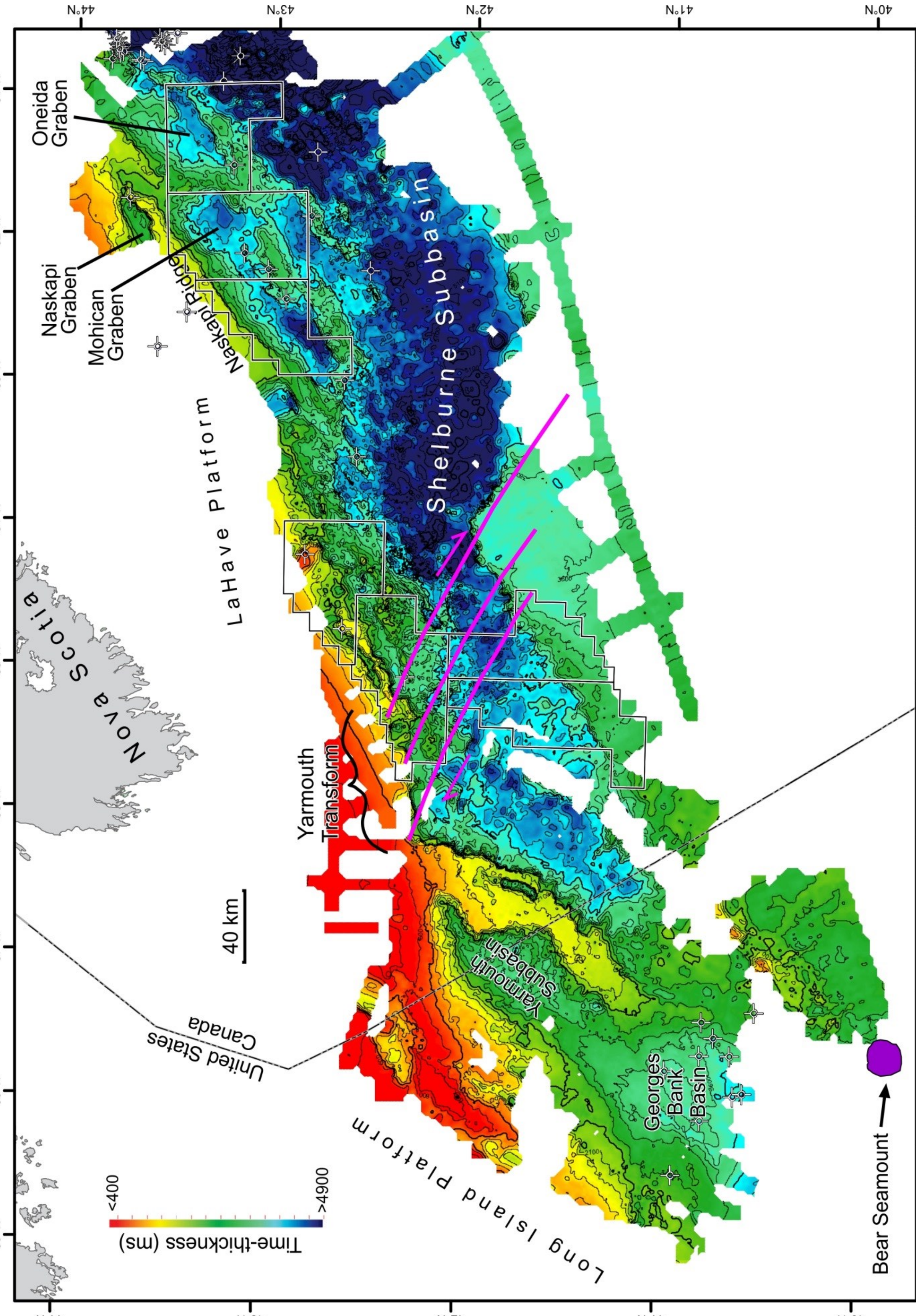

Figure 2.5 Time-thickness map between the top of crystalline basement and the seafloor.

Shelburne Subbasin, as defined by Wade and MacLean (1990), east of Georges Bank Basin (Figure 2.5). While numerous published reports are available for the geology of Georges Bank (e.g. Austin et al. 1980; Schlee and Klitgord 1988; Wade and MacLean 1990; Poag 1991; Poppe and Poag 1993), modern research east of Georges Bank has been comparatively meager. Using a combination of vintage and more recent 2D and 3D reflection seismic data-sets (see Figure 2.2 for data-coverage and a list of seismic programs used), the following discussion provides geological context for Parcels 1 to 4 and detailed description of several important structural and stratigraphic elements on this part of the margin.

Yarmouth Arch

The Yarmouth Arch is the most prominent basement element off southwestern Nova Scotia (Figures 2.3, 2.4, 2.6). It consists of a faulted and segmented basement horst block that separates the Georges Bank Basin to its west from the Shelburne Subbasin to its east. The arch forms a SSW-trending protrusion of crystalline basement that extends at least 150 km from the adjoining LaHave Platform. The 12 to 38 km wide top surface of the Yarmouth Arch is generally flat lying, except where it is offset by normal basement faults or where small volcanogenic features generate local rugosity (described below; Figures 2.6, 2.7). The structure generally narrows, is more deeply buried, and has a lower relief towards the SSW where it is more difficult to map. The Yarmouth Arch is probably composed of Early Paleozoic metasedimentary rocks of the Meguma Supergroup and associated Devonian granites that intrude them, but the basement rocks here have not been directly sampled. Early Paleozoic metasedimentary crystalline basement is confirmed on the Long Island Platform at the base of the Cost G-1 well, 90 km southwest of the Yarmouth Arch (Figure 2.4). On the LaHave Platform, the Meguma metasedimentary rock and granites have been sampled and dated from the base of the Montagnais I-94 and Mohawk B-93 wells located 120 and 175 km northeast of the Yarmouth Arch, respectively (Wade and MacLean 1990; Pe-Piper and Jansa 1999).

On aeromagnetic data, the arch produces a strong positive magnetic anomaly that closely mimics its planform shape (Figure 2.8). On gravity data it does not produce an obvious anomaly, but is flanked to the west by a gravity low generated by the Yarmouth Subbasin (described in a following section) and to the northeast by another gravity low generated by a deep basin where the Yarmouth Arch intersects the LaHave Platform (Figure 2.9). A prominent positive shelf edge anomaly (gravity high) lies to its east along much of its length. On reflection seismic profiles, the northern parts of the Yarmouth Arch are veneered by a distinctive high amplitude seismic reflection that continues beyond the edges of the arch, above more heavily deformed strata (Figures 2.7, 2.8). This surface passes laterally into an angular unconformity (collectively referred to as the J200 marker, and shown in Figure 2.6). Its reflection seismic response is similar to that produced by the ~150 m thick CAMP-related lava flows penetrated by the Glooscap C-63 well on the central Scotian Shelf and the subsurface reflection produced by buried Rhaetian age North Mountain Formation tholeiitic basalts in the Fundy Basin. Contiguous with this reflection are a series of positive relief mounds clustered around the northern parts of the arch (Figures 2.4, 2.6, 2.7, 2.10). Their dimensions (< 70 to 210 ms (twt) tall and up to 4.1 km wide, at the base) and appearance are strikingly similar to Eocene volcanogenic mounds described by Magee et al. (2013) from high quality reflection seismic profiles off southern Australia. The mounded features on the Yarmouth Arch are likewise interpreted as small volcanoes or volcanic vents. Indeed, Figure 2.6 reveals a 900 m wide depression at the centre of the mound interpreted as a central vent, and like the volcanogenic mounds described by Magee et al (2013), saucer shaped reflections interpreted as subvolcanic sills are present beneath some mounds, producing internal reflections within the rocks of the Yarmouth Arch. This implies that the mounds did not simply grow above the Yarmouth Arch, as might be expected if these features were carbonate build-ups.

The strong magnetic character of the Yarmouth Arch (Figure 2.8) combined with its reflection seismic character and the presence of interpreted volcanogenic features, strongly implies that parts of the Yarmouth Arch are veneered by volcanic lava flows. Furthermore, the flows appear to extend several kilometers west and east of the arch where they overlie deformed pre-volcanic synrift stratigraphic successions or merge with the postrift unconformity. The lava flows and other volcanogenic features are tentatively interpreted to be related to the ~200 Ma CAMP episode. However, the presence of buried Middle Jurassic seamounts at the mouth of the Georges Bank Basin (Wade and MacLean, 1990), and alkalic mid-Jurassic volcanics and ash flows encountered in two Georges Bank wells (Lydonia Canyon 133 and Cost G-2; Hurtubise et al. 1987; Elliott and Post, 2012), raises the possibility that these volcanogenic features could be somewhat younger. Unfortunately the Lower and Middle Jurassic succession is highly condensed or absent above the northern parts of the Yarmouth Arch, making it impossible to discriminate the timing of these features without direct sampling.

Primary salt basin west of Yarmouth Arch

West of the Yarmouth Arch in the northeastern parts of the Georges Bank Basin is a distinct subbasin containing up to 2 sec (twt) of moderately to heavily deformed strata referred to here as the Yarmouth Subbasin (Figures 2.4, 2.5). Its general structure is a complexly faulted half-graben, with the most important border faults dipping towards the west or northwest away from the irregular western margin of the arch (Figure 2.7). The subbasin is up to 52 km wide and 115 km long, with the thickest strata located above the hanging wall adjacent to the Yarmouth Arch or near the centre of the subbasin. Strata thin more gradually towards the west and northwest, away from the arch, onto the faulted eastern parts of the Long Island Platform (*sensu* Wade and MacLean 1990).

The basin fill is complex, consisting of faulted and folded layered successions as well as deformed transparent to chaotic intervals interpreted as salt bodies. The latter are generally rooted to an autochthonous layer located above faulted basement, and range from pillows or salt anticlines to poorly developed salt stocks or walls. Some chaotic salt intervals pass laterally into folded and deformed layered successions, which could indicate that the primary salt was originally interbedded with other lithologies. Early fill above the salt is generally layered. An impressive turtle structure occupies much of the basin, with most of the salt expelled towards the Yarmouth Arch (Figure 2.7). A grid of the top salt surface shows the distribution of isolated north to northeast trending diapirs, as well as more complex salt structures that rose up along eastern border faults, adjacent to the Yarmouth Arch (Figure 2.11). In addition to turtle structures, layered successions elsewhere above the salt are also commonly folded, and an angular unconformity is present where these deformed intervals were truncated by the postrift unconformity just west of the Yarmouth Arch.

The fill of the Yarmouth Subbasin has not been penetrated by any wells, but correlation into Cost G-2 ~50 km to the south indicates that much of the early basin fill is older than the Early Jurassic(?) Argo Salt encountered at the base of this well (Schlee and Klitgord 1988; Poppe and Poag 1993). Some workers have speculated the fill of the Yarmouth Subbasin could be as old as Carboniferous, with salt corresponding to the basal Mississippian Windsor Group (e.g. Wade and MacLean 1990). However, it is equally possible the basin formed in the Permian or even in the Triassic, with the salt here being equivalent to or slightly older than the Late Triassic Osprey Formation encountered in wells on the southern Grand Banks (McAlpine 1990). Although the maximum age of the salt in the Yarmouth Subbasin cannot be known with the available data, it is clear that some of the early salt structures were later reactivated, and continued to influence sedimentation even after the postrift unconformity. Numerous faults sole out above or along the flanks of salt diapirs, offsetting Jurassic and even Lower Cretaceous strata, and at least one growth interval involving probable Jurassic strata produced a distinct 40 km long and < 5km wide north to northeast trending trough shaped salt-withdrawal basin in the northern parts of the Yarmouth Subbasin (Figure 2.10). As such, postrift salt tectonics in this basin, as with the basins east of the Yarmouth Arch, is prevalent. To the east however salt tectonism is

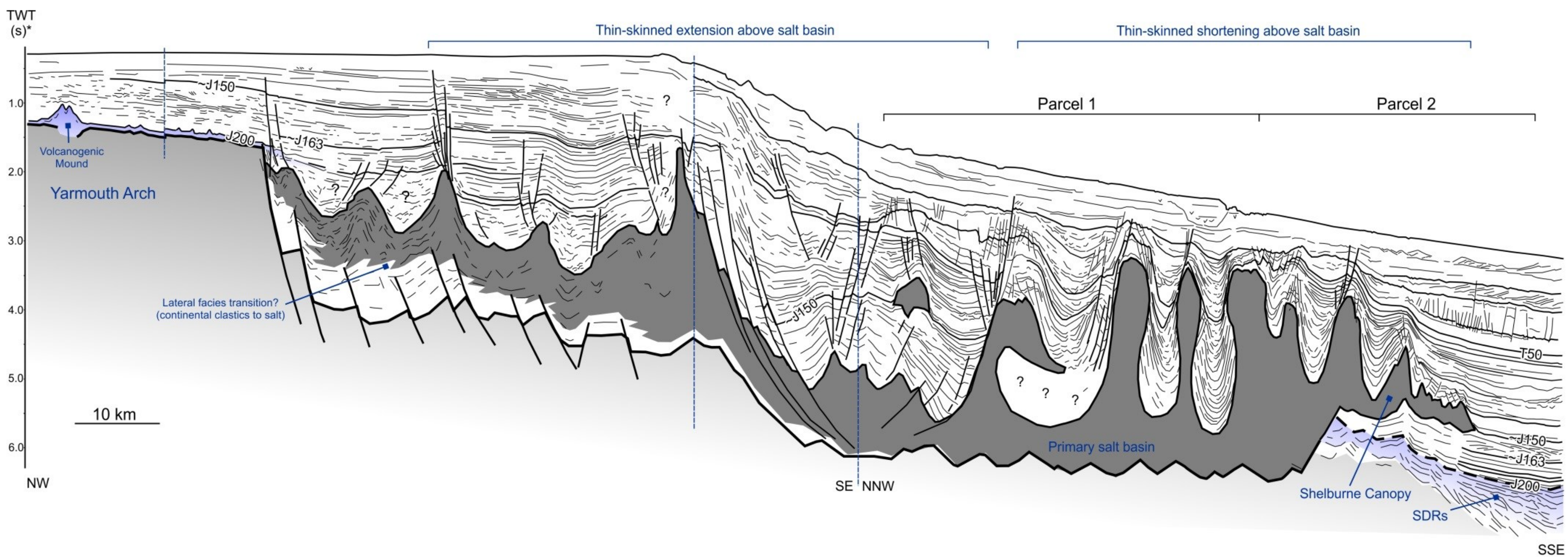

Figure 2.6. Regional composite dip transect crossing the Yarmouth Arch, and extending down the slope, across the western parts of the Shelburne Subbasin, terminating just seaward of the Shelburne Canopy, which sits above the succession of seaward dipping reflections (SDRs). Note the interpreted volcano above the Yarmouth Arch. *Note that the water column was depth converted, removing the associated velocity sag caused by increasing water depths. See Figure 2.3 for line location.

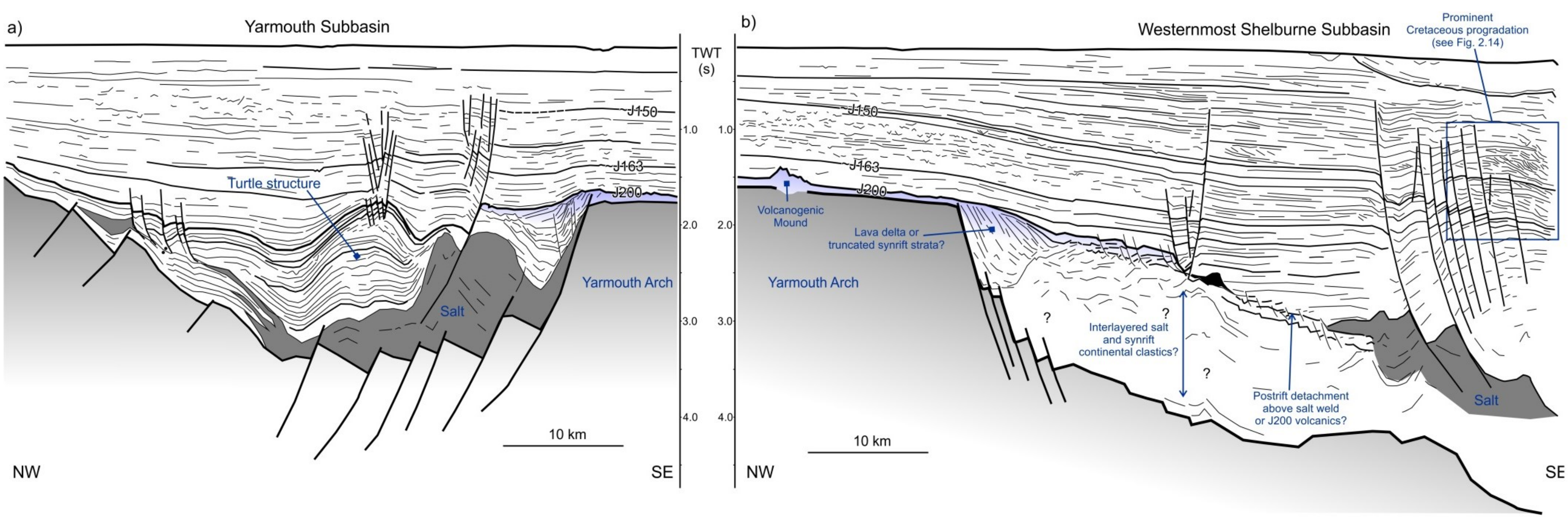

Figure 2.7. Representative transect across a) the Yarmouth Subbasin and b) the westernmost Shelburne Subbasin (Shelburne Delta). See Figure 2.3 for line locations.

more clearly linked to Late Triassic (Osprey) or earliest Jurassic (Argo) salt (e.g. Shimeld 2004; Deptuck 2010, 2011a; Kendell 2012).

Primary salt basin east of Yarmouth Arch

Another primary salt basin lies east of the Yarmouth Arch (Figure 2.11), occupying the western most parts of the Shelburne Subbasin, as defined by Wade and MacLean (1990). The salt basin corresponds, in part, to Shimeld's (2004) salt province I. Crystalline basement, and the sediments that immediately overlie it, are poorly imaged in this region. This is particularly true along a 10 to 20 km band paralleling the Yarmouth Arch, where strata show subtle discontinuous layering, with poorly defined faults and folds that cause the succession to pinch and swell (Figures 2.6, 2.7). The succession, which is capped by the J200 marker, is interpreted to correspond to Triassic rift deposits, and the undulations to poorly developed salt pillows. Further down the slope there are clear salt pillows, large salt rollers, and even rare salt diapirs, where younger faults increasingly sole out into this salt-bearing interval. Continuing down the slope, evidence for salt rising from a thick primary salt basin is unequivocal, with widespread diapirism and minibasin development (see Shimeld 2004; Deptuck 2011a).

These observations imply there is a lateral change in the dominant lithofacies with increasing distance from the Yarmouth Arch. Immature clastic-dominated Eurydice facies may pass laterally into mixed Eurydice and salt facies, and eventually into more massive salt intervals (Osprey to Argo equivalent) towards the main part of the autochthonous salt basin (landward parts of Parcels 1 and 2; Figure 2.11), where rift and early postrift subsidence were greatest. Similar lithofacies changes are recognized in the Mohican Graben on the central Scotian margin (described in a following section). The western boundary of the primary salt basin is therefore interpreted to be transitional over a 10 to 20 km region adjacent to the Yarmouth Arch (Figure 2.11).

In contrast, the seaward termination of the salt basin is a clear linear structural boundary marked on seismic profiles by an abrupt northeast-trending vertical step that forces inflated autochthonous salt to rise vertically (Deptuck 2011a) (Figure 2.6). This step appears to have formed where seaward dipping reflections (SDRs), presumed to correspond to thick intervals of basaltic lava flows interlayered with volcaniclastics, accumulated during the latest stages of rifting or earliest postrift (Larsen et al. 1994; Keen and Potter 1995; Jackson et al. 2000). In this setting, the volcanics loaded and depressed the seaward edge of the original primary salt basin that separated Nova Scotia from Morocco (Deptuck 2011a). As such, the volcanic wedges may bury parts of the salt basin and underlying continental crust. SDRs have been tracked on seismic profiles from the Bear Seamount, near the southern tip of the Yarmouth Arch, to an interpreted transform fault zone that offsets the seaward edge of the salt basin, roughly 360 km to the northeast (i.e. the Yarmouth Transform – described below).

Yarmouth Transform

Several observations infer that an important NW-SE trending strike-slip margin trends obliquely through the southwestern Scotian margin (Figures 2.4, 2.8, 2.11):

- A greater than 60 km right-lateral offset of the Yarmouth Arch relative to the edge (hinge) of the LaHave Platform immediately to its east;
- a corresponding sharp, more than 60 km right-lateral offset in the seaward limit of the autochthonous salt basin;
- the presence of an anomalously deep salt basin where the Yarmouth Arch intersects the LaHave Platform;
- clustering of volcanoes or volcanic vents along the northern parts of the Yarmouth Arch
- the abrupt change in the density, style, and distribution of salt bodies between Shimeld's (2004) salt provinces I and II; and
- the recognition of clear offsets in the East Coast Magnetic Anomaly (ECMA) that align with the offset along the seaward boundary of the primary salt basin.

The matching 60+ km right-lateral offsets in the landward versus seaward boundaries of the salt basin, in particular, implies that either a single heavily curved strike-slip boundary, or a series of smaller scale slightly curved strike-slip faults, accommodated the offset in the salt basin. A similar transfer fault has been schematically proposed by both Manspeizer (1988) and Welsink et al. (1989), but the basis for this fault is not discussed in any detail. The distribution of several en-echelon deep-seated faults identified on seismic profiles across this region implies that a wider region of strike-slip faulting accommodated the offset, rather than a single fault. Some of these faults sole out along and in some cases even offset the Moho. As such, this wider region of strike-slip faulting is similar to the situation along the southern Grand Banks (the southwest Grand Banks transform margin described by Pe-Piper and Piper 2004).

We herein refer to this strike-slip accommodation zone as the Yarmouth Transform Fault Zone (or the Yarmouth Transform for short), and similar to Manspeizer (1988) and Welsink et al (1989) interpret it as a splay coming off the South Atlas fault zone (see figure 3.1 of Manspeizer 1988 and figure 20 of Welsink et al. 1989). Right-lateral offset across the curved Yarmouth Transform helps explain the more northerly-trending basement grain to its west (including the Yarmouth Arch), compared to the dominantly northeast basement fabric to its east. A small amount of clockwise rotation south of the transform re-aligns the basement fabric on both sides of the transform (Figure 2.5).

Postrift Salt Tectonics

Postrift cover strata west of the Yarmouth Transform form a thin-skinned linked system above the primary salt basin, characterized by a landward extensional domain and a seaward compressional domain (Figure 2.6). A time-structure map along the top Jurassic seismic marker (J150) shows the location of thin-skinned extensional faults in the landward part of this system (Figures 2.12, 2.13). They extend in an arc that parallels the Yarmouth Arch continuing into the western parts of the Mohawk Graben Complex. Salt rollers dominate this region, but locally salt diapirs are also present. The profile in Figure 2.6 crosses a more salt-rich region immediately adjacent to the northern part of the Yarmouth Arch where clear downbuilding and extensional growth faulting took place. One salt diapir in this proximal region rises nearly to the seafloor (just out of the plane of the seismic section). A profile further to the southwest shows a series of tightly spaced faults that sole out along a salt weld and within the landward parts of the primary salt basin (Figure 2.7). Salt expulsion from this region appears to have driven by gravity spreading in an area of increased sedimentation associated with the Shelburne Delta (Wade and MacLean 1990). This delta system was long lived with numerous transgressive-regressive cycles recorded in Middle Jurassic to Upper Cretaceous strata, across these growth faults. The clearest progradation, however, appears to be within Cretaceous strata above the J150 marker (region identified in Figures 2.13, 2.14).

The density of salt diapirs increases down the slope. Downbuilding above the main part of the autochthonous salt basin appears to have produced a series of minibasins separated by complexly deformed salt diapirs. Isolated salt stocks and more elongated salt walls are generally rooted to the primary salt layer (Shimeld, 2004). Many of these salt bodies were reactivated and squeezed well into the Cenozoic, and salt overhangs and pinched stems are common (Figure 2.6). Seaward of the salt basin is a 10 to 25 km wide and ~85 km long salt tongue canopy referred to as the Shelburne Canopy (Deptuck, 2011a). It was expelled up and over the SDRs, advancing most rapidly across the paleo-seafloor in the Middle to Upper Jurassic (right side of Figure 2.6). It ceased its seaward advance at the end of the Jurassic, and today sits immediately above the ECMA (Figure 2.11). Its timing is similar to the Banquereau Synkinematic Wedge on the eastern Scotian Slope (Deptuck et al. 2014).

Unlike the gravity spreading system to the west (where sedimentation rates were high), salt tectonics east of the Yarmouth Transform were driven primarily by gravity gliding in response to margin tilting, and not sediment loading (Deptuck 2010, 2011a). The landward parts of the salt basin here are dominated by slabs of Jurassic and to a lesser extend Cretaceous cover strata that detached and slid down the slope above salt pillows and salt rollers, or a primary salt weld. This

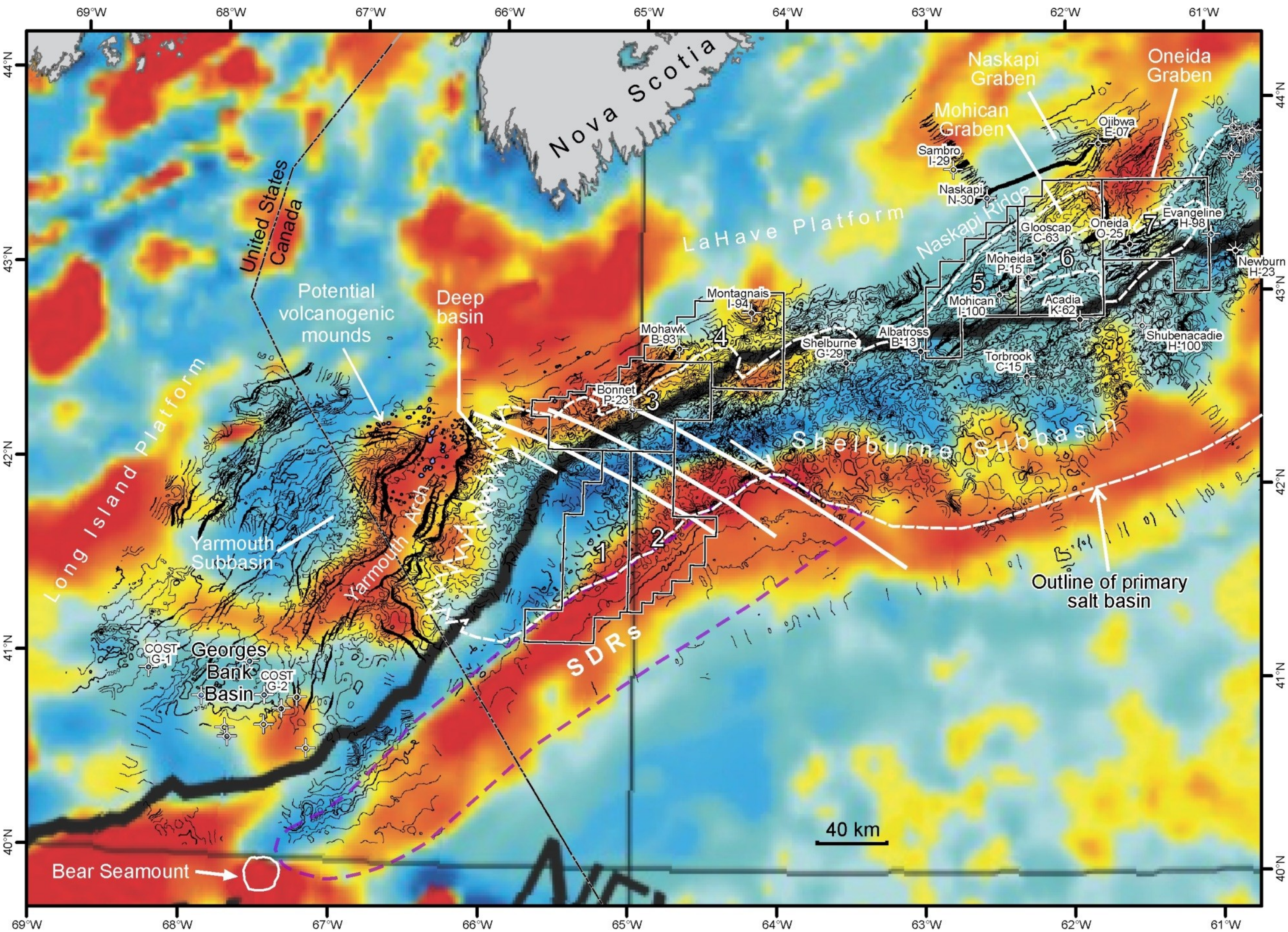

Figure 2.8 Magnetic anomaly map overlain by key structural elements, including major basement faults and the top basement contours (250 ms spacing). Magnetics data from Oakey and Dehler (2004).

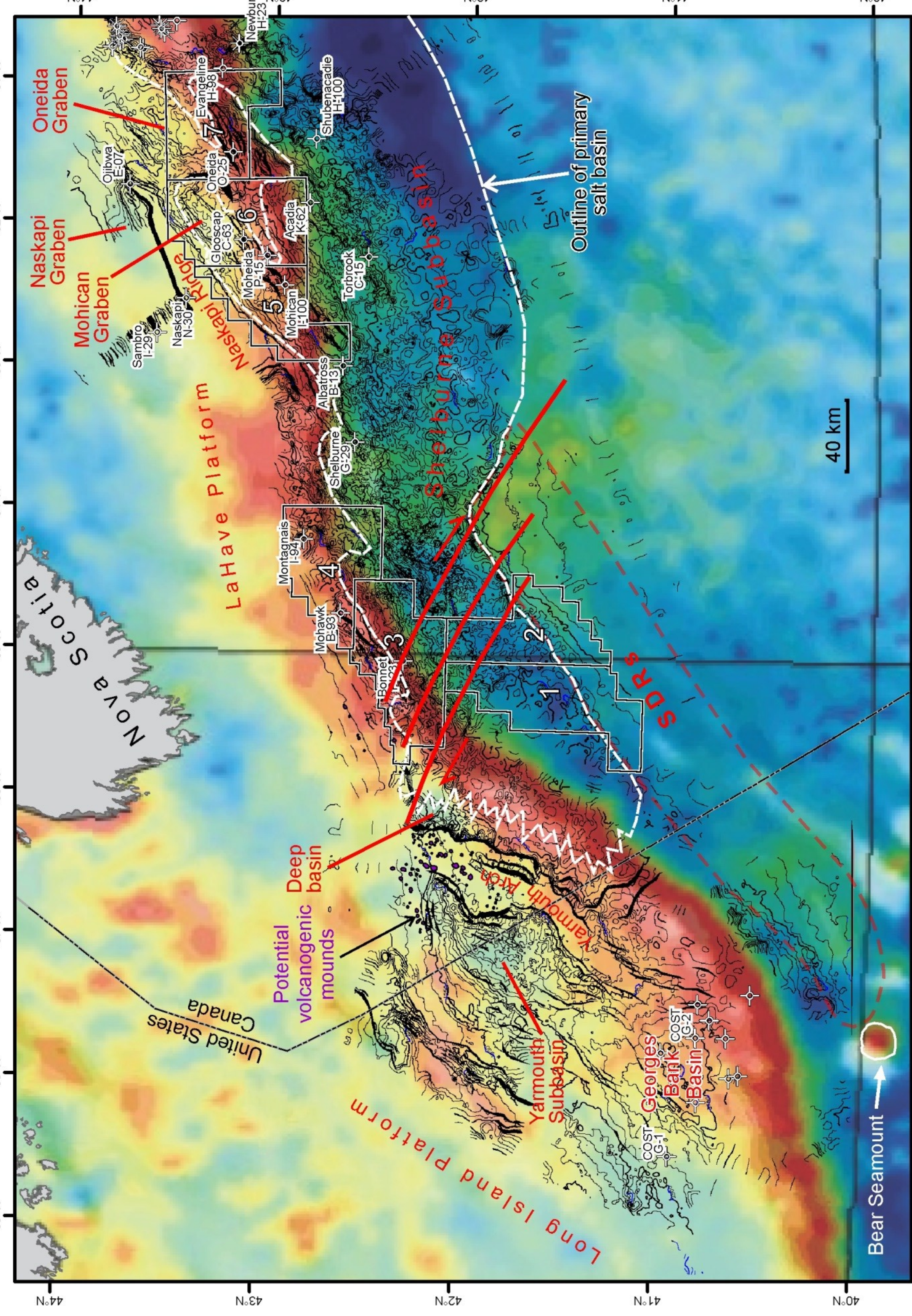

Figure 2.9. Gravity anomaly map overlain by key structural elements, including major basement faults and contours from top basement (250 ms spacing). Gravity data from Dehler and Roest (1998).

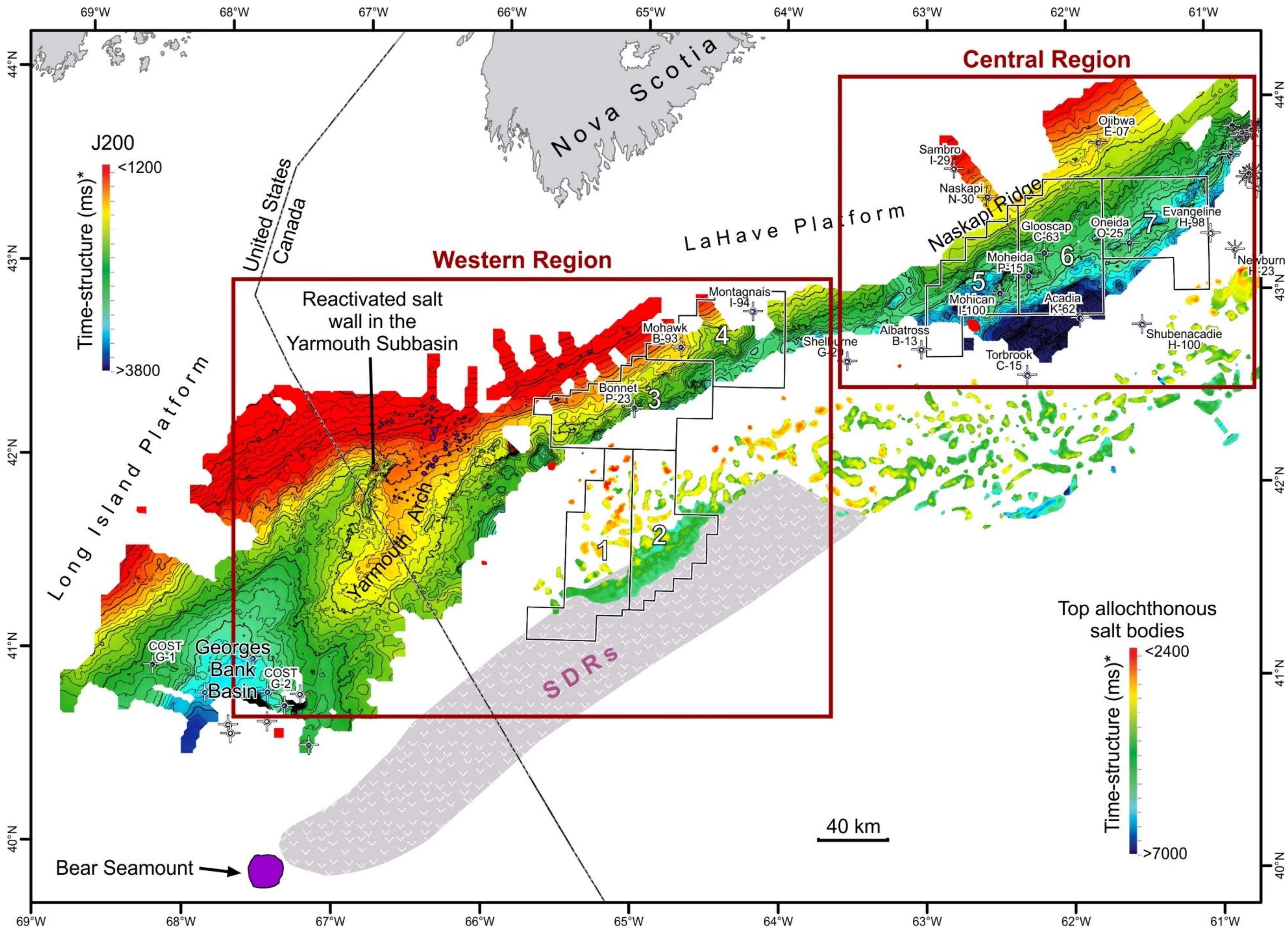

Figure 2.10 Time-structure map of the postrift unconformity, merged with a strong reflection that, in the central region corresponds to CAMP-related basalts (calibrated at Glooscap C-63) and in the southwestern region is uncalibrated, but is contiguous with a number of small volcanogenic features identified on seismic profiles. The surface is highly diachronous, but is interpreted to separate pre-CAMP strata below from post-CAMP strata above. *Note that the water column was depth converted, removing the associated velocity sag caused by increasing water depths.

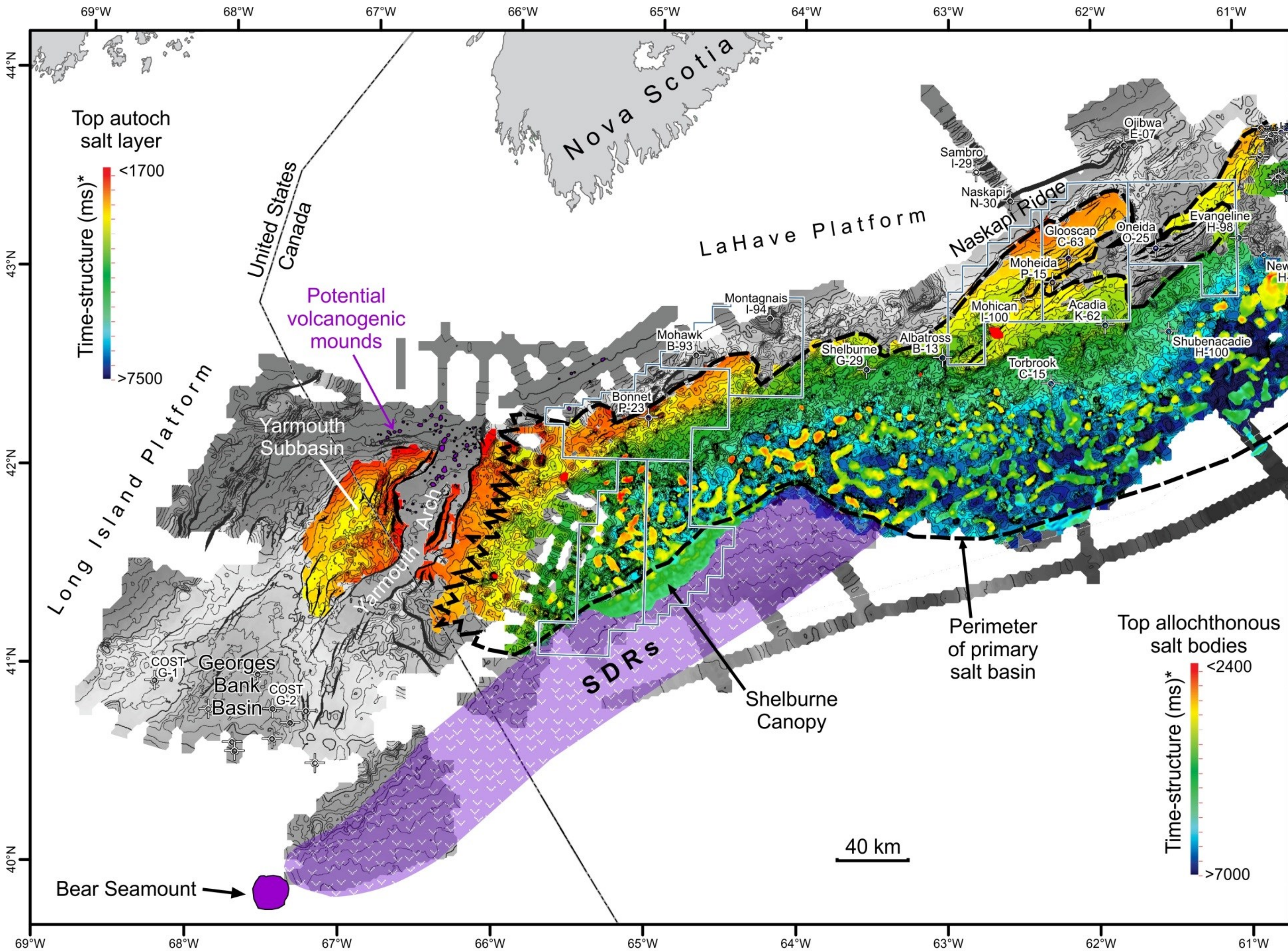

Figure 2.11 Time-structure map of the top surface of the autochthonous salt layer, overlain by the top surface of allochthonous salt bodies. Dashed line shows approximate perimeter of the Late Triassic primary salt basin. *Note that the water column was depth converted, removing the associated velocity sag caused by increasing water depths.

produced the 'slope detachment province' (Deptuck 2011a), which continues along the slope east of the Yarmouth Transform for approximately 350 km. Taller salt stocks and walls are generally restricted to the slope seaward of this region, where downbuilding within subcircular to elongated minibasins expelled salt from the thickest parts of the primary salt basin. A detailed account of the salt tectonics east of the Yarmouth Transform is presented in Deptuck (2011a).

Parcel Description and Exploration Potential

Parcels 1 and 2 are located entirely on the slope in water depths ranging from approximately 1050 to 3100 m and above the primary salt basin that lies seaward of the Yarmouth Arch. The Shelburne Delta is located immediately landward (northwest) of these parcels. Numerous complex salt diapirs and walls, expelled in the Jurassic to mid-Cenozoic, can be found in the landward parts of Parcels 1 and 2. In contrast, the Middle to Late Jurassic Shelburne Canopy occupies the seaward parts of these parcels (Figure 2.6). No wells have been drilled in either parcel, but numerous hydrocarbon trap configurations are possible. Traps may include salt-cored folds, three-way closures on salt flanks, and traps associated with turbidite sands beneath, and sealed by, the Shelburne Canopy as it advanced seaward. Turbidite sands derived from the Shelburne Delta are the most likely reservoirs. Tentative correlation into Cost G-2 and Mohawk B-93 implies that progradation of the Shelburne Delta began in the Middle Jurassic (above the J163 marker), with numerous regressive-transgressive cycles recognized up into strata as young as Late Cretaceous. The best developed delta clinoforms are found in Cretaceous strata above the J150 marker (Figure 2.14), particularly beneath the northeastern parts of Georges Bank (Figure 2.13). As such, the most reservoir prone intervals in Parcels 1 and 2, immediately downslope of the Shelburne Delta, are probably Cretaceous.

Further north, Parcels 3 and 4 are located on the outer shelf and upper slope in water depths ranging from approximately 100 to 1700 m. The landward parts of these parcels are positioned above the Mohawk Graben Complex, in an area with poor seismic coverage. The grabens form narrow but deep (up to 1.4 sec twt) basins presumed to contain synrift fluvial-lacustrine strata equivalent to the Eurydice Formation, capped by the J200 surface. The western parts of the Mohican Graben Complex may also contain salt (western half of Parcel 3), but detailed mapping is not possible here. Above the Mohawk Graben Complex, the Middle to Late Jurassic and earliest Cretaceous succession is characterized by mixed carbonates and clastics that were deposited above the Mohawk Graben Complex. Bonnet P-23 is the only test of the Middle to Upper Jurassic carbonate bank west of Albatross, more than 150 km away. It was drilled about 6 km back from the highly faulted reef margin and encountered a variety of lithologies in the Baccaro: shaly limestones, dolomites and dolomitic limestones. Near the base of the Baccaro a number of thick dolomite intervals were penetrated with good porosities and loss circulation zones, but no hydrocarbons were encountered, possibly due to lack of fault seal. The northern edge of the Barrington 3D survey extends onto the outer parts of the carbonate bank (Figure 2.12), where local carbonate build-ups are recognized in the eastern part of Parcel 3. One of these has very bright amplitudes which could signal porosity development, hydrocarbon charge, or both. Other portions of the bank edge show rim development, but the lack of 3D seismic makes these difficult to map.

In addition to carbonates, Middle to Upper Jurassic siliciclastic reservoirs are also possible in these parcels. Mohawk B-93 encountered a 505 m thick texturally mature sand-dominated Upper Jurassic succession, of which 194 m were porous sands averaging 23% porosity (Given, 1977). Although it is not possible with the existing dataset to delimit any traps in the landward parts of Parcels 3 and 4, acquisition of modern 3D seismic volumes may reveal new closures associated with compaction above basement horst blocks or even fault blocks within the synrift succession, in addition to potential carbonate-related targets.

Significant portions of Parcels 3 and 4 are located seaward of the margin hinge zone (and carbonate bank edge) and within the 'slope detachment province'

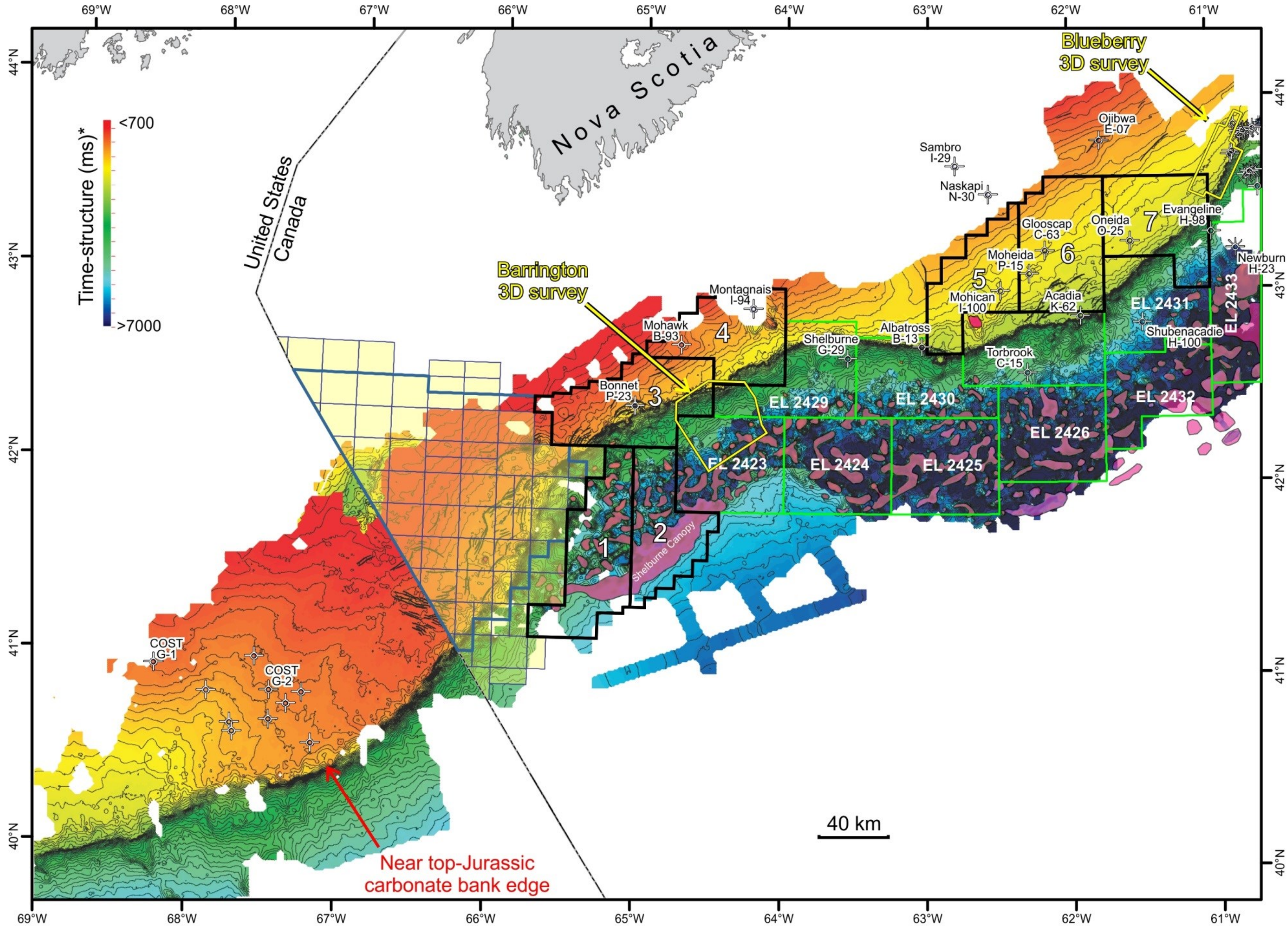

Figure 2.12 Time-structure map of the J150 marker (or where absent, the correlative top Jurassic surface) above the top autochthonous salt surface, showing the distribution of the carbonate bank edge. Allochthonous salt bodies are identified in pink and are mostly found seaward of the carbonate bank edge. *Note that the water column was depth converted, removing the associated velocity sag caused by increasing water depths.

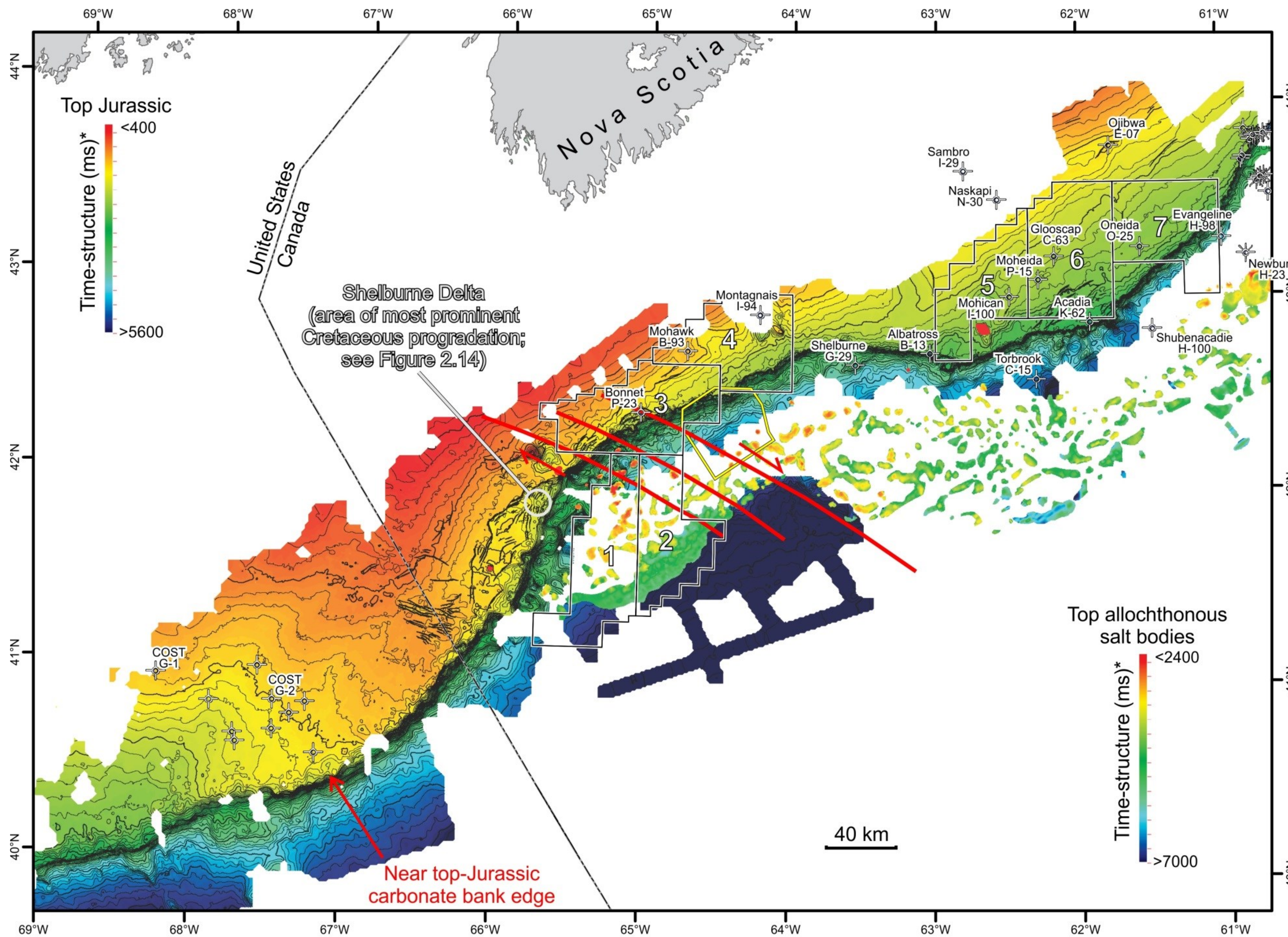

Figure 2.13 Time-structure map of the J150 marker (or where absent, the correlative top Jurassic surface) showing the distribution of the carbonate bank edge. The top allochthonous salt grid is overlain on this map (salt bodies mostly found seaward of the carbonate bank edge). *Note that the water column was depth converted, removing the associated velocity sag caused by increasing water depths.

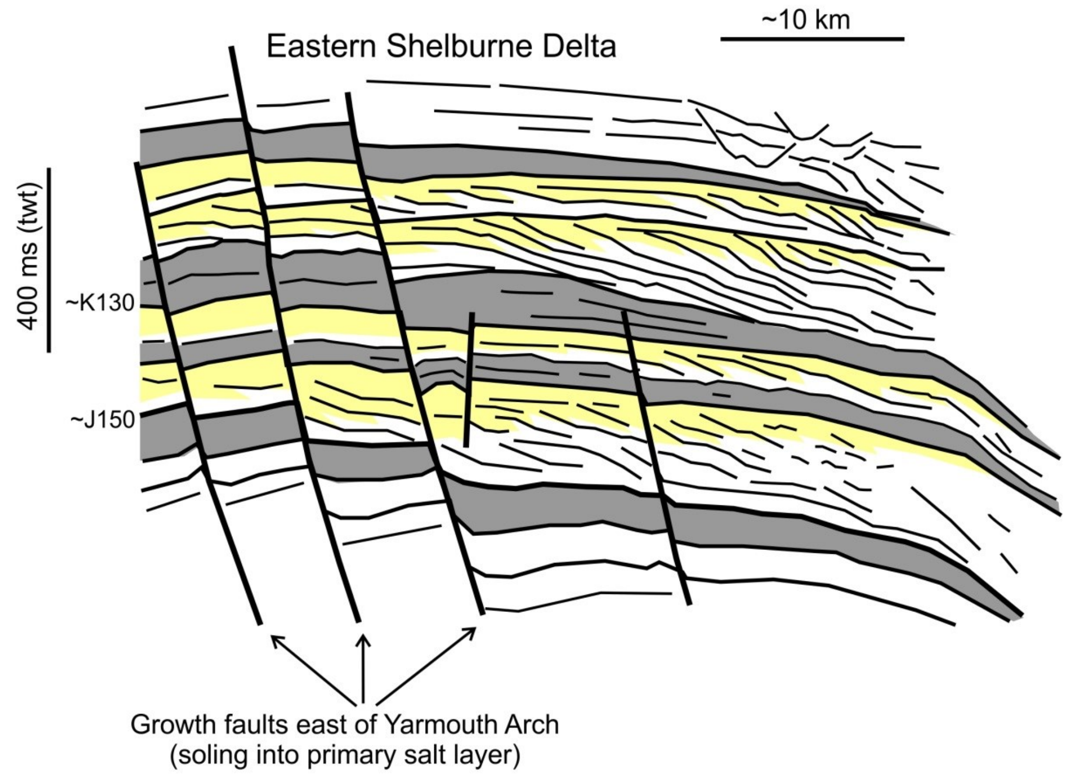

Figure 2.14 Line drawing interpretation from a seismic profile presented in MacDonald (2011) across the eastern Shelburne Delta, showing multiple stacked Cretaceous transgressive (grey) and regressive (yellow) cycles above the J150 marker, immediately west of Parcels 1 and 2.

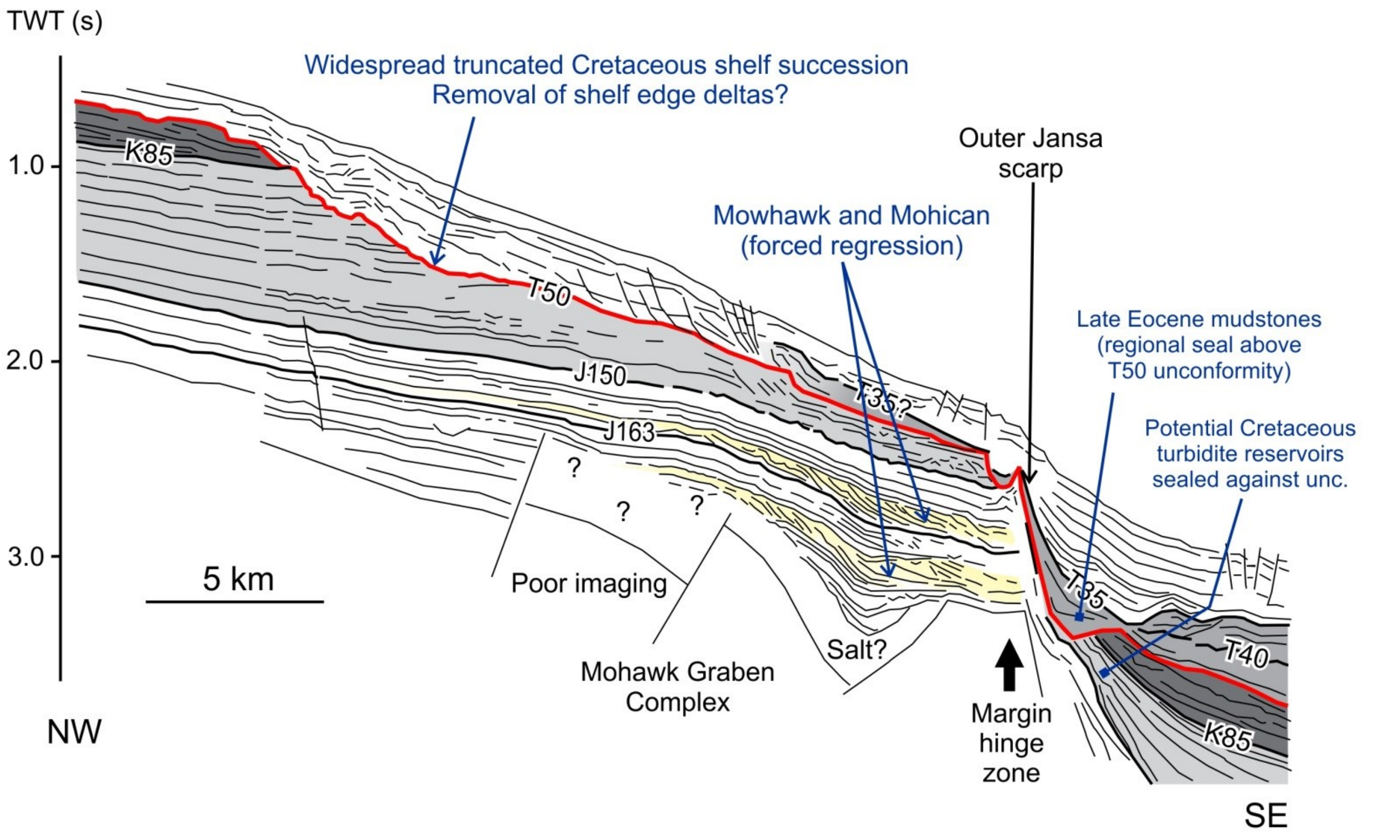

Figure 2.15 Seismic profile line drawing from the outer part of the LaHave Platform, seaward of Mohawk B-93, showing widespread erosion along the T50 marker (red) and potential for an unconformity trap developed where Late Eocene shales drape the T50 truncation surface. Note also two intervals of progradation (interpreted as forced regressions) that probably delivered sand to the Jurassic slope.

described by Deptuck (2011a) (Figures 2.12, 2.13). Seismic profiles indicate that the texturally mature sand-dominated Upper Jurassic succession at Mohawk B-93 correlates seaward into the topsets of a Callovian or Oxfordian shelf-edge delta (forced regression - Figure 2.15) in what must have been a gap in the carbonate bank. The eastern parts of the Shelburne Delta may also have extended onto Parcels 3 and 4. Widespread erosion of Cretaceous shelf strata during the Montagnais marine impact event, however, has removed the outer shelf succession east of the most obvious Cretaceous Shelburne Delta clinoforms (e.g. Figures 2.15, 2.16, 2.17, 2.18, 2.19) (see also Deptuck and Campbell 2012). That the Middle to Upper Jurassic and potentially even Cretaceous shelf-edge deltas delivered sand to the slope in Parcels 3 and 4 is supported by time-thickness maps in deepwater and amplitude extractions from the Barrington 3D survey (Figure 2.20). These extractions show clear evidence for submarine channel systems in Jurassic, Cretaceous and Tertiary strata, indicating that multiple turbidite reservoir intervals are possible off southwestern Nova Scotia.

Potential reservoirs could have been incorporated into a number of structural and stratigraphic traps. Potential structural traps involve Jurassic to Earliest Cretaceous strata rotated and detached as rafts above the autochthonous salt layer, and their raised edges may locally form traps draped by younger Cretaceous strata. The most promising targets, however, are stratigraphic traps in the seaward parts of Parcel 3 and 4 where turbidites onlap the slope or where turbidite sands were truncated by the T50 unconformity and later draped by widespread Eocene mudstones, creating unconformity traps (e.g. Figure 2.15).

One potential stratigraphic trap is the Cayuga lead captured in the Barrington 3D survey (Figures 2.21, 2.22). It consists of a series of mid-Cretaceous to Early Eocene amplitude anomalies interpreted to correspond to turbidite channel reservoirs contained within a combination up-slope pinch-out and angular unconformity trap. Cayuga is found immediately down-slope from the eroded carbonate bank edge ('outer Jansa Scarp' of Deptuck and Campbell, 2012), partly overlapping Shell's exploration licenses 2423 and 2429. Two main intervals produce anomalous amplitudes that terminate up-slope and down-slope. Amplitude extractions from the lower interval show a clear network of channels converging down-slope into trunk channels. The associated amplitude anomaly covers an area of about 290 km^2 and terminates where it onlaps the steep foreslope of the Jurassic carbonate bank (Figures 2.21, 2.22a). Amplitude extractions from the upper interval show a much broader anomaly that appears to correspond to the floor of very wide latest Cretaceous or earliest Cenozoic canyons sculpted by the Early Eocene T50 unconformity (Figure 2.22b). This amplitude anomaly could also correspond to massive reservoir units deposited during the ~50.5 Ma Montagnais impact event, or shortly after from turbulent flows carrying better sorted sand down the slope as water resurged back towards the crater cavity shortly after the initial marine impact event (see Deptuck and Campbell, 2012). The associated amplitude anomaly covers an area of about 266 km^2. Both of these amplitude anomalies stack vertically, producing a potentially very large stratigraphic trap.

A key element of this trap is the widespread Montagnais erosion surface that produces an angular unconformity all along the Outer Jansa Scarp (e.g. Figures 2.15, 2.16). This angular unconformity was subsequently draped by widespread Late Eocene mudstones (Late Eocene mudbelt/sub-unit 1c of Deptuck and Campbell, 2012), producing an important regional seal. Although there appears to be up-slope pinch-out or onlap of several of the deeper Cretaceous turbidite channels mentioned above, the presence of the angular unconformity and later regional seal reduces the risk of up-slope leakage along channels that could compromise the integrity of the stratigraphic trap. The Cayuga lead could be analogous to the Buzzard field in the North Sea, which contains 400 million barrels of oil in Late Jurassic reservoirs that form a wedge-shaped stratigraphic trap thinning onto the slope (Dore and Robbins 2005). The Jubilee discovery of Ghana containing stacked Turonian turbidites (95 m of pay; ~700 mmboe recoverable) may also be an appropriate analogue.

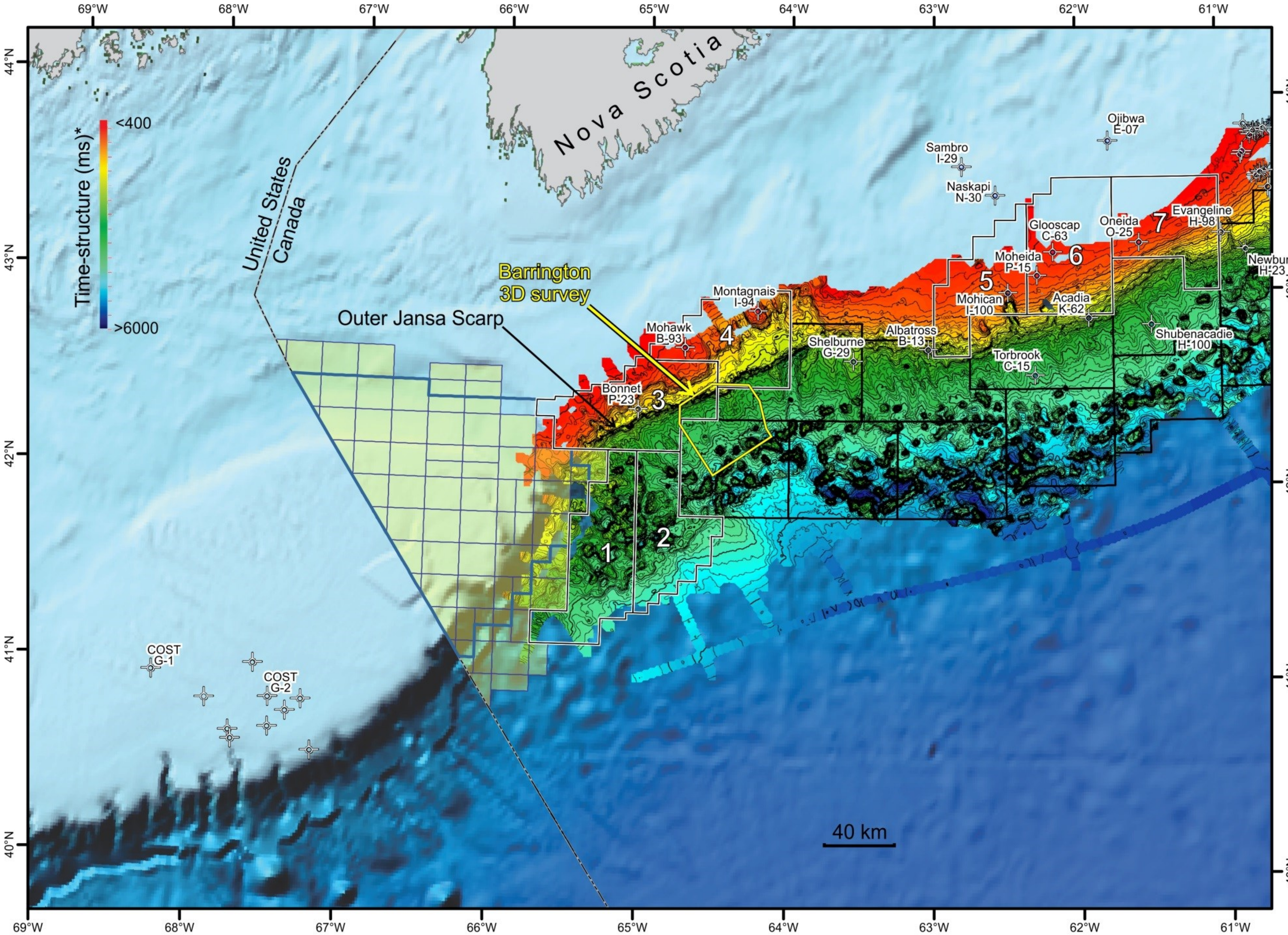

Figure 2.16 Time-structure map of the T50 marker, a widespread unconformity produced by the ~50.5 Ma Montagnais bolide impact (see Deptuck and Campbell, 2012). *Note that the water column was depth converted, removing the associated velocity sag caused by increasing water depths.

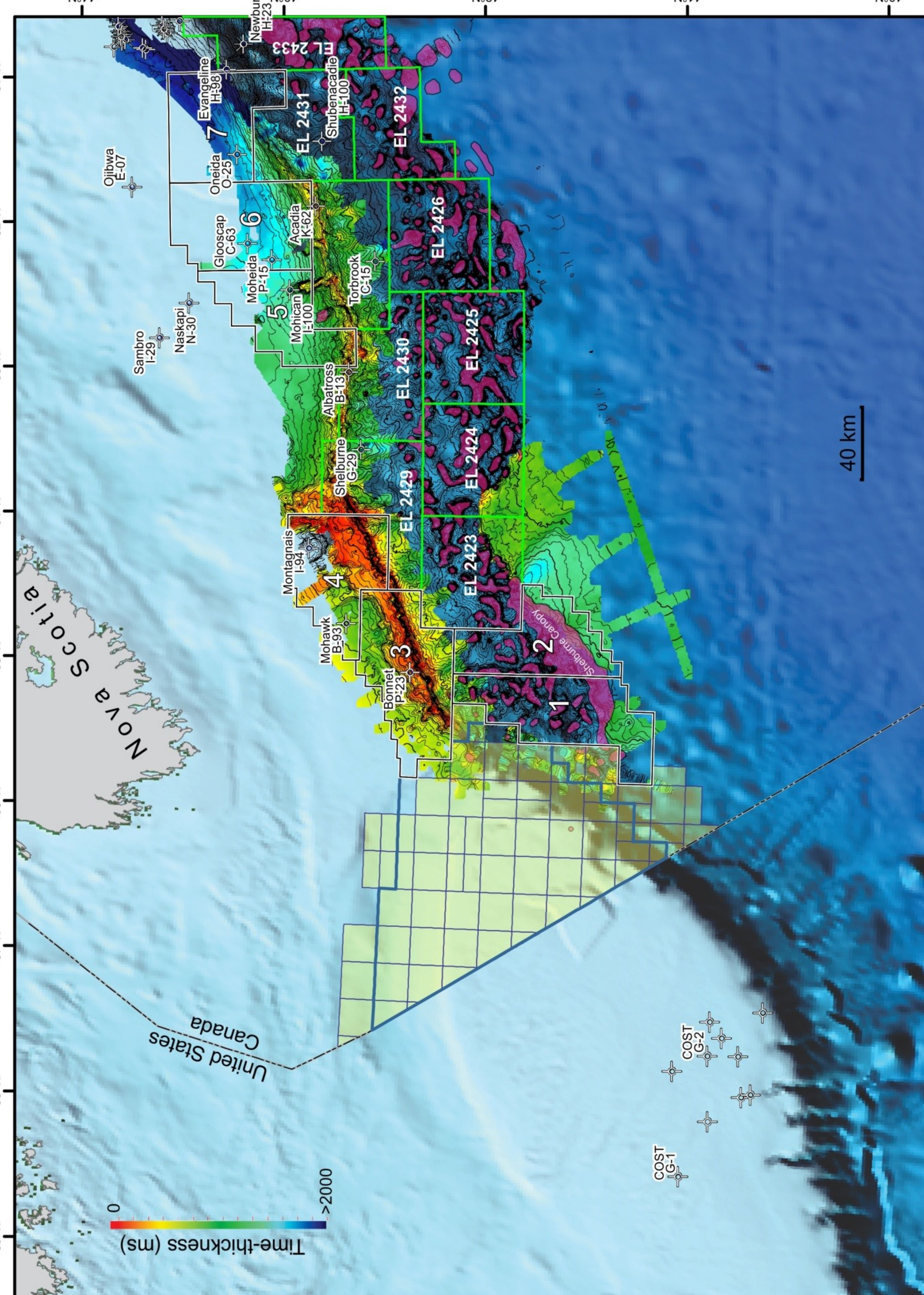

Figure 2.17 Time-thickness map between J150 and T50, showing the widespread erosion of Cretaceous to Paleocene strata adjacent to and seaward of the Montagnais impact crater (see Deptuck and Campbell, 2012).

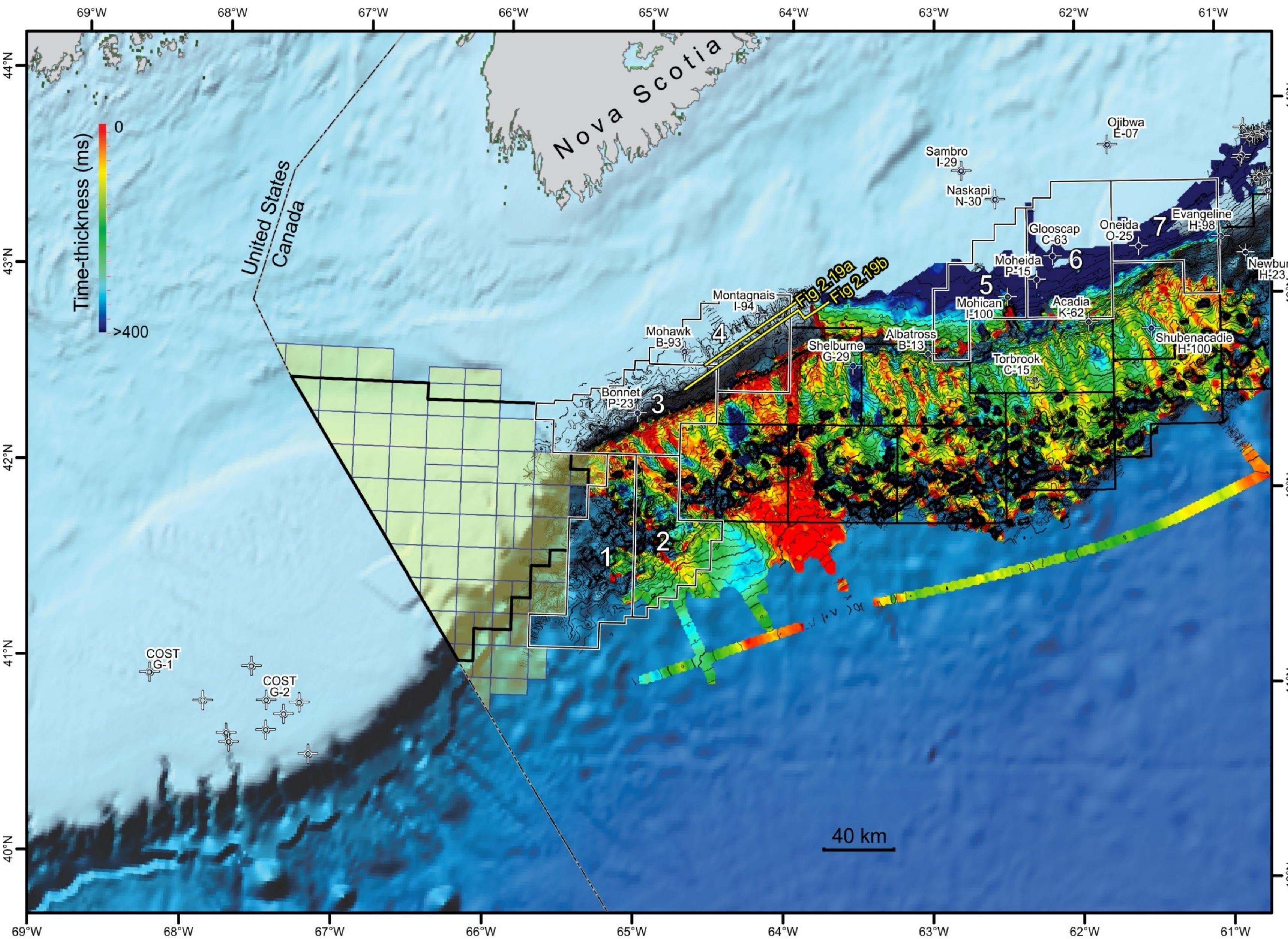

Figure 2.18 Time-thickness map between K85 and T50, draped above the T50 structure contours, showing the widespread erosion of Upper Cretaceous to Paleocene strata adjacent to and seaward of the Montagnais impact crater (see Deptuck and Campbell, 2012).

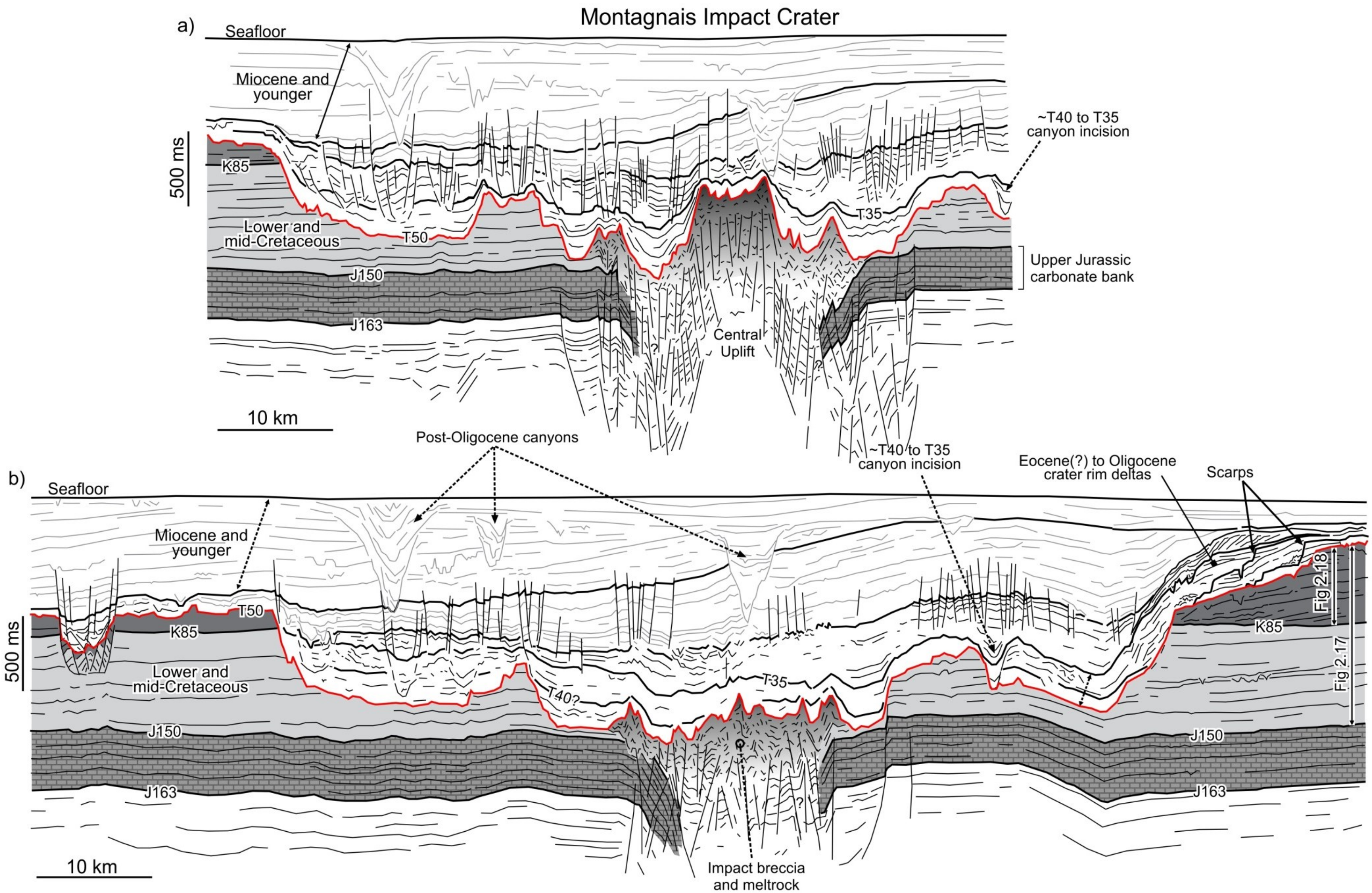

Figure 2.19 Line drawings of seismic profiles crossing the Montagnais impact crater, showing central uplift draped by impact breccia and meltrocks (calibrated at Montagnais I-94) and widespread erosion along the T50 unconformity in red (modified from Deptuck and Campbell, 2012). See Figure 2.18 for line locations.

Numerous similar amplitude anomalies are recognized on 2D seismic profiles both west and east of the Barrington 3D survey in Parcels 3 and 4, as well as seaward into Parcels 1 and 2 where they onlap salt structures, implying that potential turbidite onlap traps could be widespread. In addition, shallower stratigraphic traps associated with younger Cenozoic turbidites that onlap the steep slope are also possible, and a wide variety of amplitude anomalies that could be DHIs are present in Parcels 1 to 4 (e.g. Castel lead identified in Figure 2.21). As Torbrook C-15 has shown, however, some of the shallowest amplitude anomalies could correspond to poorly consolidated low-velocity siltstones (Kidston et al., 2007).

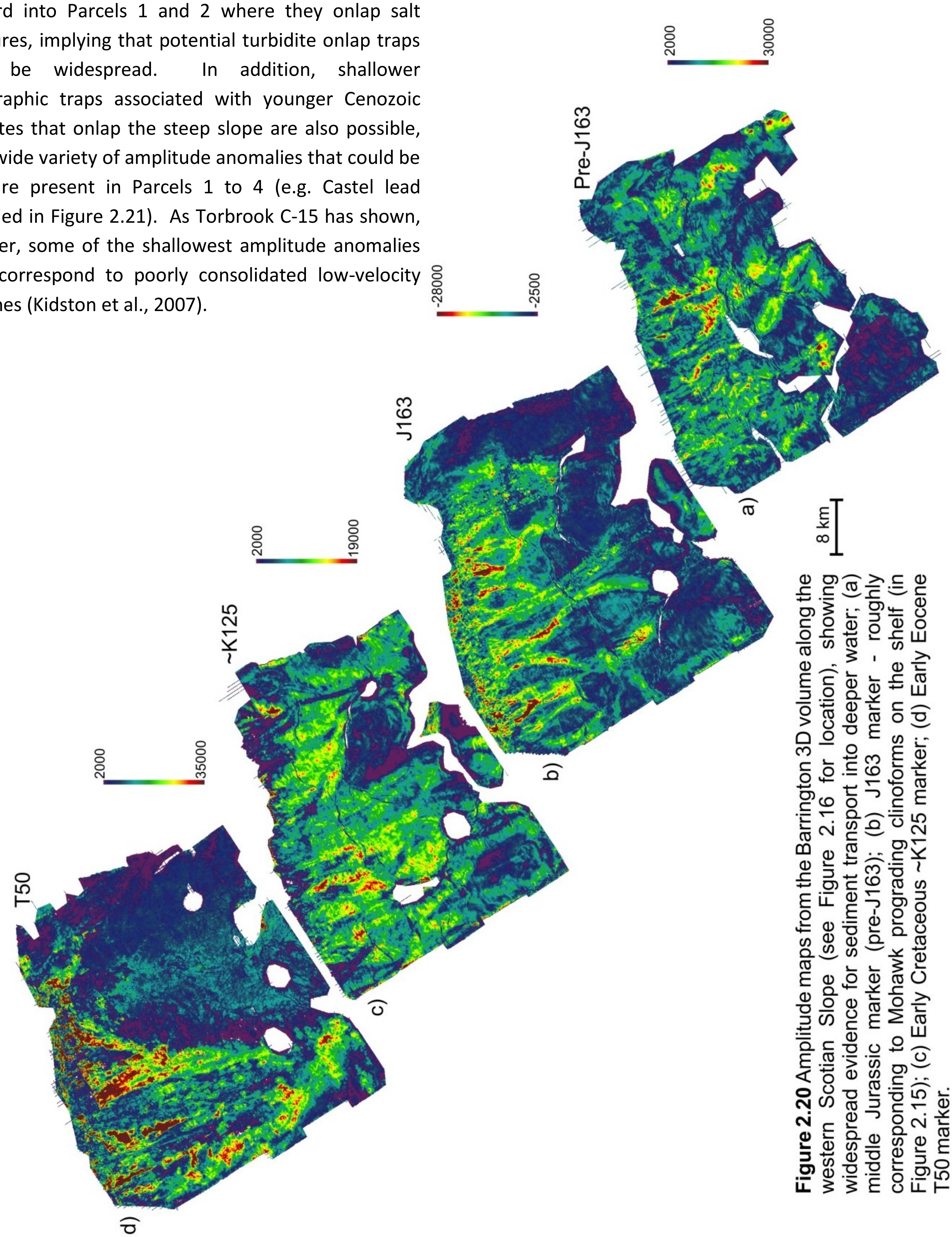

Figure 2.20 Amplitude maps from the Barrington 3D volume along the western Scotian Slope (see Figure 2.16 for location), showing widespread evidence for sediment transport into deeper water; (a) middle Jurassic marker (pre-J163); (b) J163 marker - roughly corresponding to Mohawk prograding clinoforms on the shelf (in Figure 2.15); (c) Early Cretaceous ~K125 marker; (d) Early Eocene T50 marker.

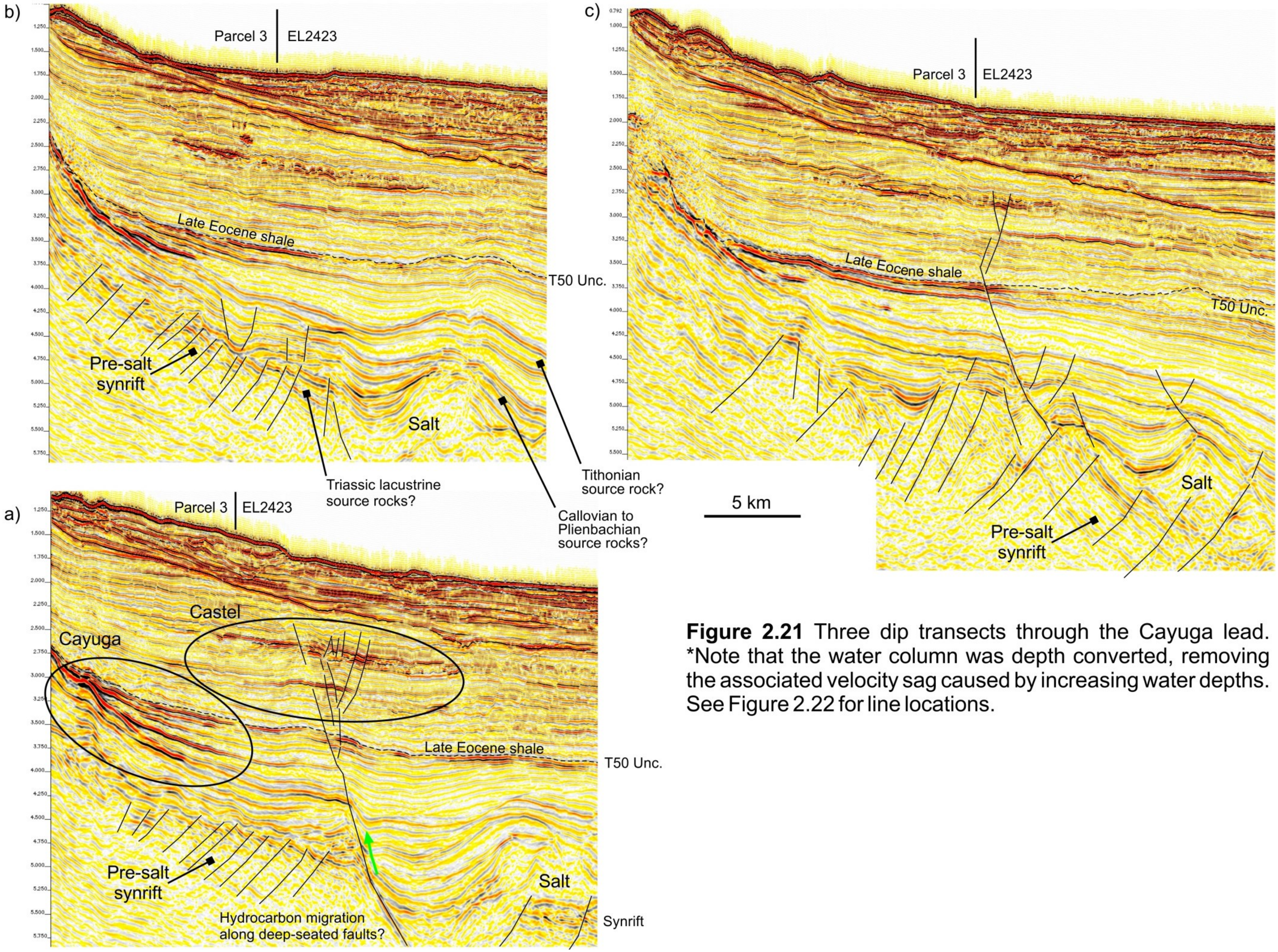

Figure 2.21 Three dip transects through the Cayuga lead. *Note that the water column was depth converted, removing the associated velocity sag caused by increasing water depths. See Figure 2.22 for line locations.

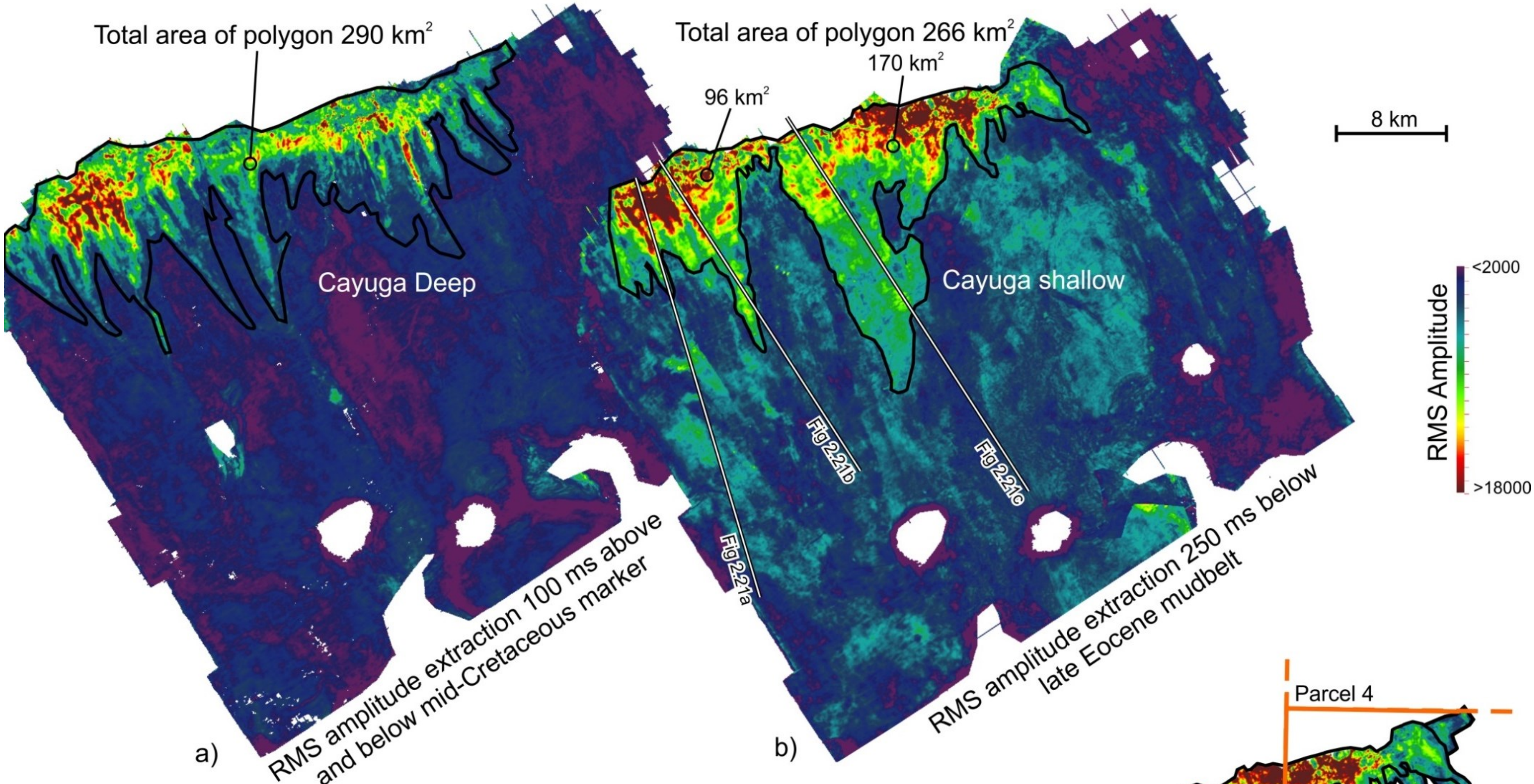

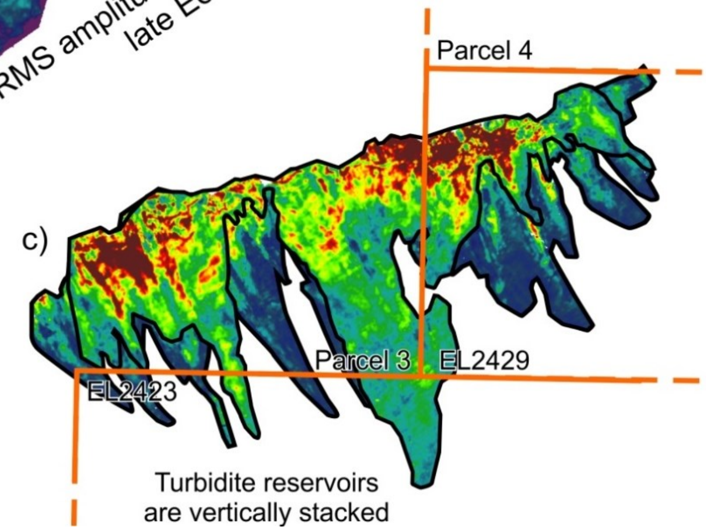

Figure 2.22 RMS amplitude extractions from the Barrington 3D volume, showing a) Cayuga deep - amplitude anomalies associated with mid-Cretaceous turbidite channels that onlap the steep foreslope of the Jurassic carbonate bank; b) Cayuga shallow - amplitude anomalies along the floor of broad erosive canyons formed during the Montagnais bolide impact, draped by widespread late Eocene mudstones; c) Cayuga shallow and Cayuga deep stacked vertically.

3. Central Region

Exploration History

The central part of the Scotian margin has been somewhat better explored than the western area, with four wells included with Parcels 5, 6, and 7 (Figure 1.1, 2.2) and an additional five wells located nearby. The eight wells tested several play types, though they encountered no significant petroleum shows.

In the Central region, exploration began in the late 1960s on the shallow water Scotian Shelf as an extension of the activity around Sable Island to the east. Following a number of seismic programs, five wells were drilled in the 1970s to early 1980s to test structural plays. A sixth well tested a shallow rollover anticline in the mid-1980s, and then interest turned to the deep water slope with two wells testing stratigraphic and structural traps. Following extensive, basin-wide regional 2D seismic surveys in the late 1990s, the slope region was licensed by industry though resulting only in a single well drilled in 2003 to test a shallow stratigraphic play. No significant oil and gas shows were encountered in any wells.

Oneida O-25 (1970) was the third well drilled in the Scotian Basin. It was operated by Shell to test a very large (~225+ km^2) unfaulted, low relief simple anticlinal closure on the LaHave Platform. Closure was mapped at the top Jurassic (Abenaki / Baccaro). Beneath the stratigraphic succession was a very large northeast-southwest trending tilted basement ridge with its northern edge defined by a northwest-dipping normal fault with considerable offset. The target horizons were the Cretaceous and Jurassic intervals. The Cretaceous Logan Canyon and Missisauga formations were shale dominated with a few large porous but wet sands. The Jurassic Abenaki Formation was an oolitic limestone and shale succession with minor sands, all of which were tight with only a few porous intervals. No hydrocarbon shows or zones were discovered in any of the units and the well abandoned at 4106 m TD in Mohican Formation sandstones and dolomites.

Mohican I-100 (1972) is a key well on the western Scotian Basin as it penetrated a near complete Late Tertiary to Late Triassic stratigraphic succession and recovered nine conventional cores from potential reservoir intervals. It was drilled by Shell on the outer edge of the Scotian shelf in 153 m water to test a large simple four-way closure above a low relief salt pillow as defined by the top Jurassic seismic horizon. A thick shale-dominated upper Tertiary (Pliocene-Miocene) section was first penetrated that unconformably overlies a thin Late Cretaceous section. This was followed by a thick Late to Middle Jurassic succession that had surprisingly little porosity. For the Abenaki Formation, this could be facies-related as the limestones were mostly mudstones with few oolitic or other grainstone lithologies. The early Jurassic Iroquois Formation sandstones and dolomites were tight with the latter invariably anhydritic. At the base of the well, the approximately Sinemurian age Breakup Unconformity is underlain by a thin (79 m) interval of Late Triassic redbeds followed by 28 metres of Argo Formation salts. There were no hydrocarbon accumulations or significant shows in any of the strata penetrated and the well ended at 4388 m TD in Argo salts.

Petro-Canada **Moheida P-15** (1977) was drilled in close proximity (~20 km NE) of Mohican I-100 in 112 m water. It too was designed to test potential dolomite reservoirs in the Early Jurassic Iroquois Formation in a simple structural closure above a basement feature. This large (~83 km^2) elongate feature was defined by a seismic horizon interpreted as the top Iroquois. The well was drilled on the feature's crest and encountered a similar stratigraphic succession to I-100 but with a thicker Cretaceous interval. The Late Cretaceous Logan Canyon Formation was shale dominated and while much thinner, the Missisauga Formation was capped with a thick porous fluvial sandstone though with no shows. The underlying Late Jurassic Abenaki Formation was composed mostly of lime mudstones but with better developed oolitic grainstones though the latter were tight. Some modest porosity was present in the targeted Iroquois Formation sandstones though the dolomites were tight. The postrift unconformity at 3848 m capped the remaining 445 m of Mohican to Eurydice Formation tight redbed sediments in which the well ended at 4293 m. No hydrocarbon shows were present in the well.

Chevron-Petro-Canada-Shell **Acadia K-62** (1978) was drilled to test a low-relief, narrow, elongate, bank-edge structural closure delineated by seismic. Closure was mapped on the footwall at the top of the Jurassic (Baccaro Mb.) that relied on closure against the main hingeline down-to-the-basin fault. The initial section penetrated was a thick (~2400 m) Tertiary shale succession. A mid-Cretaceous and later lower Tertiary unconformities removed most of the Cretaceous sediments with only ~450 m of Dawson Canyon Formation and younger mudstones remaining. K-62 drilled a complete Abenaki Formation section (Roseway, Baccaro, Misaine, and Scatarie members). Except for the Misaine, the carbonate members were composed of various oolitic limestone lithologies with generally fair to very good porosity. The top Roseway had considerable dolomitization with very good intercrystaline porosity. The expected dolomites of the Early Iroquois Formation were not penetrated (i.e. were deeper) but instead a mixed succession of oolitic grainstones, sandstones and shales of the Mohican Formation with fair to good porosity in the carbonates. No oil staining or significant mud-gas shows were encountered in the well though three DSTs were run in the Abenaki but recovered only formation water. Well TD was at 5287 m in Aalenian to Bajocian age Mohican limestones.

Shell was the first operator to drill on the deep water Scotian slope, with their **Shubenacadie H-100** well located in 1476.5 m water depth. This well falls outside the Call parcels but has relevance to plays in the deep water portions of Parcels 5 and 6. The well was designed to test an interpreted Eocene turbidite fan deposit on the paleoslope with a shallower (Miocene) seismic amplitude anomaly as a secondary target. The prognosed Miocene bright spot secondary target was encountered at 2636 m MD and consisted of 25 m of tight, very fine-grained, silty sandstone with no shows. The age of this sand is believed to be Early Pliocene rather than Miocene. Unfortunately, the sonic and density log readings across this zone are questionable due to poor hole conditions (washout). However, the resistivity logs, sidewall cores and cuttings all indicate that the zone is tight. The well's primary target zone consisted of early Tertiary to Late Cretaceous age shale, tight limestone and marl. No reservoir quality sands were encountered though four conventional cores were cut. The well was drilled to a TD of 4200m MD reaching the Middle Cenomanian upper Logan Canyon equivalent. Subsequent mapping has indicated that the interpreted fan was an erosional remnant below the Base Tertiary (Paleocene to Eocene) unconformity. The Shubenacadie structure is one of the larger remnants separating two divergent channel-dominated areas, which contributed to it resembling a constructional fan on the older seismic. The main exploration implication, also confirmed in the earlier Shelburne G-29 well, was that the Tertiary fan play remained tested.

Husky-Bow Valley **Glooscap C-63** (1984) was designed to test a ~50 km^2 drape closure over a basement high in the Mohican Graben in 122 m water. The feature relied on some modest fault seal on the eastern flank that is defined on horizons interpreted as the tops of the Scatarie Member, Iroquois and Eurydice formations. The primary target horizons were siliciclastics and dolomites of the Middle-early Jurassic Mohican and Iroquois, and Late Triassic Eurydice formations. Secondary targets were within the shallower Abenaki (carbonate) and Logan Canyon (siliciclastic) formations. The Tertiary (Banquereau Formation) and Cretaceous (Wyandot, Dawson Canyon, Logan Canyon and Missisauga formations) units were present as prognosed and there were few reservoir quality sands in the latter formation. The underlying Abenaki Formation limestones were also tight, and sandstones of the Mohican and Iroquois formations had some fair porosity. A surprise was the presence of 152 m of tholeiitic basalts of earliest Jurassic age at the postulated top Eurydice Formation and beneath this salt of the Argo Formation. Thus the well results (and later seismic mapping) revealed the interpreted basement feature was in fact a salt pillow of Late Triassic age. C-63 was devoid of any hydrocarbon shows and thus terminated at 4542.5 m in Argo Formation.

Husky-Bow Valley next drilled **Evangeline H-98** (1984) to evaluate a shallow anticline along the edge of the shelf in 174 m of water. The structure is a narrow, elongate rollover anticline with fault-dependent closures mapped at the interpreted top Logan Canyon Formation (~29 km^2 closure) and near top Naskapi Member (~48 km^2 closure). Potential gas reservoirs were expected in the fluvial-shallow marine sandstones of the lower Logan Canyon (Cree Member) and upper Missisauga formations. After penetrating the Tertiary and Late Cretaceous Wyandot Formation chalks, the well entered a thick succession of shales and siltstones of the Dawson Canyon and Logan Canyon formation. No significant sandstone reservoirs were encountered, however two gas and high gravity oil (condensate) shows were found in the Logan Canyon Formation equivalent (Cree Member). The uppermost (4022-4070 m) was found in a Late Cenomanian age MFS interval of fossiliferous, sandy lime mudstones with total gas units ranging from 1000-3300 TGU with associated oil (condensate) in drilling mud. The deeper show was in fractured shales (4801-4802 m @ 1400 TGU) accompanied by a drilling break. When compared to the seismic profiles it appears likely that this interval intersected a large listric fault. The well did not reach the targeted Missisauga Formation and was ended at 5044 m and was not tested.

The Petro-Canada **Albatross B-13** well (1985) was drilled on a pronounced structural high at the edge of the Abenaki bank margin on the deep water Scotian Slope in 1341 m water. Like Shubenacadie H-100, this well also falls outside the Call parcels but has relevance to plays in the deep water portions of Parcels 5 and 6. The feature is a long (14 km), narrow (~1.5 km) closure with an estimated 250 m vertical relief mapped at the top Abenaki (Baccaro). It is sealed on the seaward side by a basin-dipping normal fault. Target horizons within the Abenaki Formation were defined by high amplitude reflections interpreted to be porous oolitic and reefal carbonate reservoirs. Beneath the thick (~1000 m) of Tertiary age Banquereau Formation mudstones about 1200 m of Abenaki Formation carbonates were penetrated, with most of the Cretaceous succession removed by Tertiary erosion events. The upper half of the formation was composed of oolitic grainstones some of which were dolomitized. Poor to fair porosity was common in this section but with no significant shows. Two mud gas peaks of ~100 TGUs were recorded at 3434-3440m and 3012m with partial loss circulation occurring over the sections but DSTs were not attempted. The basal half of the Abenaki was mostly tight lime mudstone though with some good porosity in several dolomitic zones. The well went through about 100 m of the Callovian Misaine Member shales and siltstones and ended at 4047.5 m TD.

EnCana **Torbrook C-15** (2003) was the most recent well drilled in the western half of the Scotian Basin and was the third well in the region to test the Tertiary fan play on the deep water Scotian Slope (1675 m water depth). The primary target was an interpreted Miocene-aged turbidite channel/fan system fed from sediments on the shelf via canyons and deposited in a paleotopographic low. The secondary target was interpreted as an older Miocene fan complex. Two of the canyon feeder systems were identified at the Mohican I-100 and Moheida P-15 well locations updip on the shelf and correlated with the Late Paleogene (Middle Oligocene) relative sea level fall. Both channel/fan systems were defined by amplitude anomalies on 2D seismic. No hydrocarbon bearing reservoir quality sands were encountered in the well. Encana's primary target was penetrated at 2855 m and consisted of poorly consolidated siltstone and shale/claystone that generated a minor mud-gas response of 50-80 TGU. The secondary target was encountered at 2958 m and consisted of thin, tight, siltstone with no shows. The well ended at 3600 m in early Tertiary sediments. The post-drill interpretation was that that the anomaly was a classic slump feature with no related submarine fan deposition. It is most likely the chaotic internal nature of the slumped mass gave rise to signal attributes that while interpreted as a fan bore no relationship to potential reservoir facies.

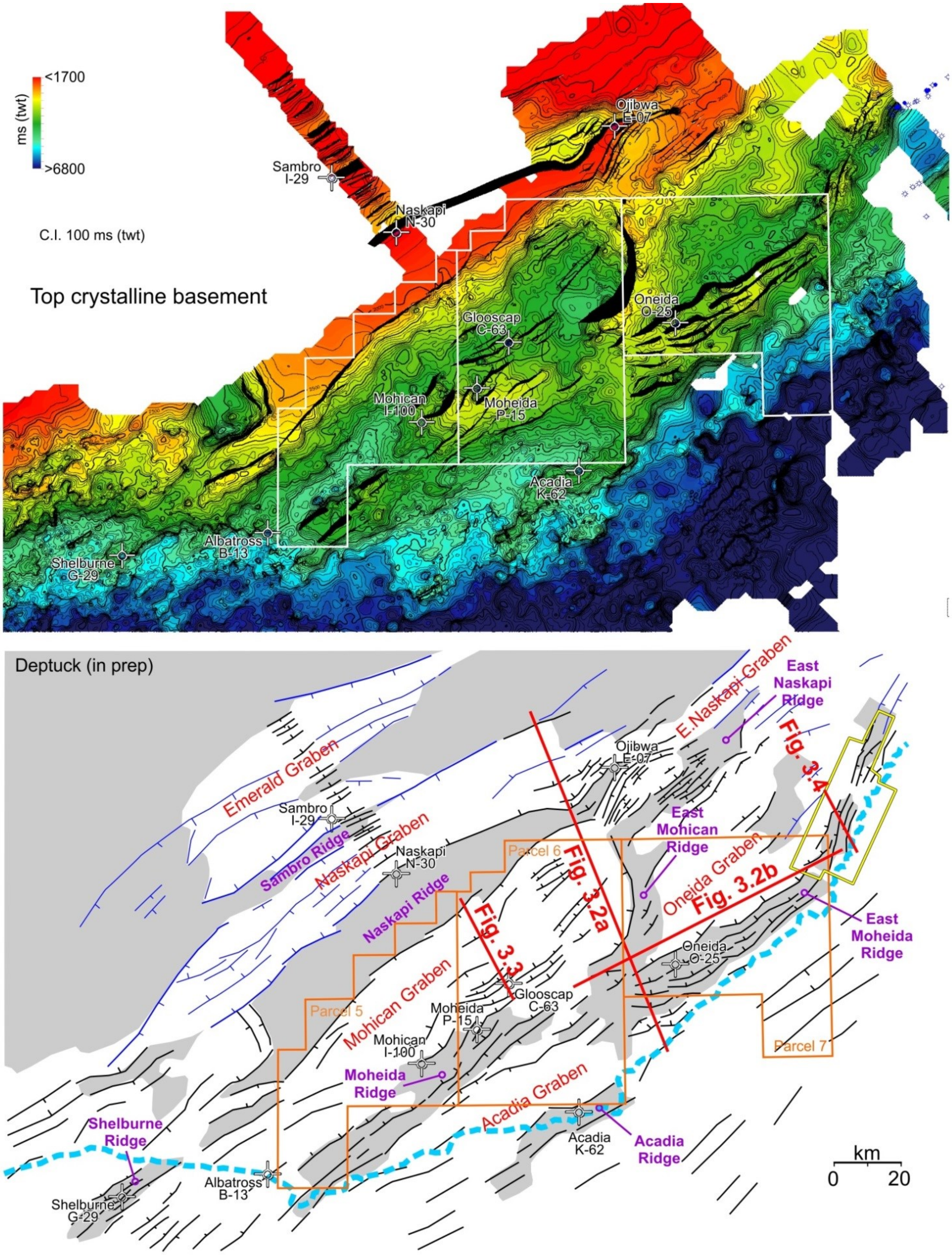

Figure 3.1 . a) Time-structure map of the top of crystalline basement in the Central region. b) Corresponding map showing important basement elements. Faults in blue are from Wade and MacLean (1990). Line locations shown in red. Blue dashed line shows the overlying Upper Jurassic carbonate bank edge. *Note that in (a) the water column was depth converted, removing the associated velocity sag caused by increasing water depths, particularly seaward of the modern shelf edge.

Geological Setting

The Central region described here is located west of the Sable Subbasin, above the heavily faulted nose of the LaHave Platform, extending onto the central Scotian Slope (Figure 1.1, 2.1, 3.1). This area is dominated by two main geologic features - extensional, locally salt-bearing rift basins that formed as Nova Scotia rifted and ultimately broke apart from Morocco, and a widespread Middle to Upper Jurassic carbonate platform that aggraded above these rift basins after continental break-up. Recent efforts have focused on more careful mapping of the top of the crystalline basement and the distribution and character of synrift strata. This work provides a clearer view of basement architecture as well as the structural development of rift basins. Several important structural and stratigraphic elements characterize this region, and are described in more detail below to provide geological context for NS15-1 Call for Bids Parcels 5, 6, and 7.

Basement Architecture

The LaHave Platform along the Central region of the Scotian margin is broken by a complex arrangement of faults that offset Early Paleozoic crystalline basement and produce synrift depocentres separated by basement highs (Welsink et al. 1989; Wade and MacLean, 1990). The dominant structural grain is northeast-southwest, and most faults (both major border faults and minor intrabasinal faults) dip landward, towards the northwest. Many of the border faults sole into landward dipping to sub-horizontal mid-crustal detachments or shear zones (e.g. Figure 3.2; Welsink et al. 1989), similar to several other rift basins of the Newark Supergroup (e.g. Manspeizer, 1988). On reflection seismic profiles, these produce horizontal to steeply inclined highly reflective intervals within the crust that can commonly be correlated over distances of many tens of kilometres. Although the typical absence of a strong, consistent impedance contrast between crystalline basement and overlying synrift strata makes correlation of a 'top basement' surface challenging, careful mapping guided by some of the better quality surveys provides a clearer view of a number of basement elements that are defined below (Figure 3.1).

The **Naskapi Ridge** is the most prominent basement element in the Central region. It forms a 4 to 22 km wide northeast-trending flat-topped basement high composed of Early Paleozoic rocks with little or no internal reflectivity. It can be followed easily along strike over a distance of 160 km. Its southwestern end terminates where it plunges sharply to the southwest into a poorly defined (crossed by only 3 seismic profiles) but deep rift basin (up to 1.6 sec twt). Its northeastern end is narrow and is heavily faulted near Ojibwa E-07, where its trajectory curves slightly to the north over its final 20 km. Here it separates faults that dip landward from those that dip seaward in what appears to be an important relay or accommodation/transfer zone. The northern edge of the Naskapi Ridge was penetrated by Naskapi N-30, which encountered Paleozoic metasedimentary rocks that probably correspond to the Meguma Supergroup (Pe-Piper and Jansa 1999). The northeastern termination of the horst block was penetrated at Ojibway E-07, which encountered Middle Paleozoic granites. Similar granites widely intrude Meguma metasedimentary rocks on mainland Nova Scotia (Jansa and Pe-Piper 1999). Unlike the Yarmouth Arch, there is no distinct or consistent magnetic response across most of the Naskapi Ridge (Figure 2.8).

The Naskapi Ridge separates the **Naskapi Graben** to the north from the **Mohican Graben** to the south (Figures 3.1, 3.2, 3.3). Its northern edge corresponds to the main landward (northwest) dipping border fault(s) of the Naskapi Graben. Its southern flank is also offset by dominantly landward dipping fault (Figure 3.3). The faulted top basement surface plunges to the southeast, away from the Naskapi Ridge, until it intersects the northwest dipping border faults that flank other basement highs like the **Moheida Ridge** (Figure 3.1). The Moheida Ridge and the **East Moheida Ridge** that is offset from it (right-lateral) are structurally much more complicated than the Naskapi Ridge. They do not consist of a single basement element, but are instead characterized by a complex jumble of faulted basement blocks and synrift strata that are challenging to unravel.

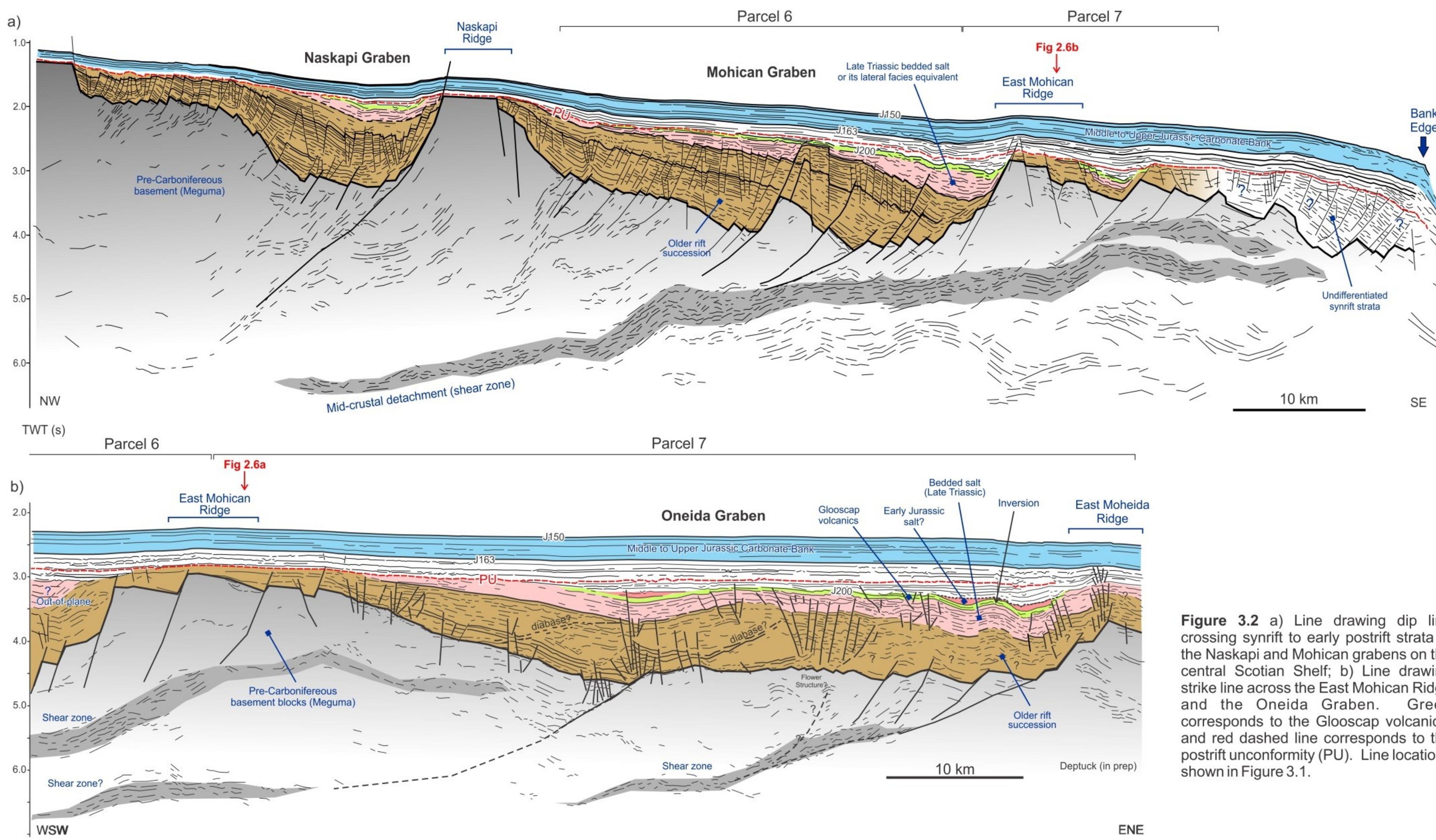

Figure 3.2 a) Line drawing dip line crossing synrift to early postrift strata in the Naskapi and Mohican grabens on the central Scotian Shelf; b) Line drawing strike line across the East Mohican Ridge and the Oneida Graben. Green corresponds to the Glooscap volcanics, and red dashed line corresponds to the postrift unconformity (PU). Line locations shown in Figure 3.1.

Figure 3.4 from the Blueberry 3D survey (CNSOPB program number NS24-E043-004E) crosses the eastern parts of the East Moheida Ridge. It shows that the ridge is cored by an elevated basement element, but clear synrift strata within a series of rotated fault blocks overlie this elevated basement element. A similar situation exists near Glooscap C-63, Moheida P-15, and Mohican I-100 that were all drilled above or off the flanks of the Moheida Ridge (Figure 3.1). Each of these wells bottomed in younger rift successions that veneer more heavily faulted older (and unpenetrated) rift intervals of unknown composition or age. It is unlikely that early synrift deposits would have accumulated above topographically elevated basement blocks, thus we infer that the Moheida and East Moheida Ridges were developed sometime after rift extension and associated sedimentation had already begun. Such features could represent inversion structures. The **Acadia Ridge** and **Shelburne Ridge** have a similar character. On gravity data, the Moheida and East Moheida ridges align with very strong positive anomalies that are commonly found along the shelf edge (Figure 2.9; Keen et al. 1990). The Acadia and Shelburne ridges, located seaward of the shelf-edge anomaly, also produce an elevated gravity response.

In contrast to the common northeast-southwest grain of most basement elements, the **East Mohican Ridge** trends normal to this orientation. It consists of an arcuate basement element that is roughly perpendicular to the Naskapi and Moheida/East Moheida ridges. Both the dip and strike profiles in Figure 3.2 cross this important basement element, showing that synrift strata both thin and are heavily eroded across it. The East Mohican Ridge produces a moderately strong positive gravity anomaly (Figure 2.9). Basement depth increases abruptly to its west, across one or more prominent basement faults with a total throw of at least 1.5 sec (twt). These faults define the eastern boundary of the Mohican Graben. The eastern flank of this high plunges more gradually beneath the **Oneida Graben** (Figures 3.1, 3.2b). The East Mohican Ridge aligns with right lateral offsets observed between Moheida and East Moheida ridges (at its southern termination) and the Naskapi and East Naskapi ridges (at its northern termination; where there is a clear relay ramp). This implies that the East Mohican Ridge developed along a right-lateral transfer zone.

Synrift to Early Postrift Structure and Stratigraphy

In the landward portion of Figures 3.1 and 3.2a, a prominent angular unconformity separates underlying synrift strata and eroded basement elements (like the Naskapi Ridge) from later onlapping and draping postrift reflections. This erosional surface corresponds to the time-transgressive 'postrift unconformity' widely described in most of the Newark-style rift grabens across offshore eastern United States and Canada (e.g. Grow et al. 1983; Manspeizer 1988; Hutchison and Klitgord 1988; Poag, 1991). On the central Scotian Shelf, strata below this surface were penetrated in Glooscap C-63, Moheida P-15, and Mohican I-100 – all in the Mohican Graben – and further landward at Sambro I-29 (Figure 3.1).

Glooscap C-63 encountered a 152 m thick interval of tholeiitic basalt flows that is geochemically indistinguishable from CAMP-related basalts like the North Mountain Basalt exposed along the shores of the Fundy Basin (Wade and MacLean, 1990; Pe-Piper et al. 1992). North Mountain Basalts have a known age of ~201 Ma (Kontak and Archibald 2003) and hence approximate the Triassic-Jurassic boundary. The Glooscap volcanics produce a strong, distinct seismic marker that is conformable with underlying strata (Figure 3.3). It has been correlated throughout parts of the Mohican and Oneida grabens, as well as landward into the Naskapi Graben. In landward areas it has been heavily eroded by the postrift unconformity; further seaward it is commonly located 500 to 700 ms (twt) deeper than the postrift unconformity. This is because later periods of extension (an inversion) dropped the volcanic layer below the level of regional erosion.

If the postrift unconformity is carried 'low', along the conformable Glooscap volcanic reflection, a more regional surface is produced that corresponds to our J200 surface (Figures 3.3, 3.5a). This surface separates pre-CAMP strata below (Triassic and older) from post-CAMP strata above (Early Jurassic and younger). A time-thickness map between J200 and the top of

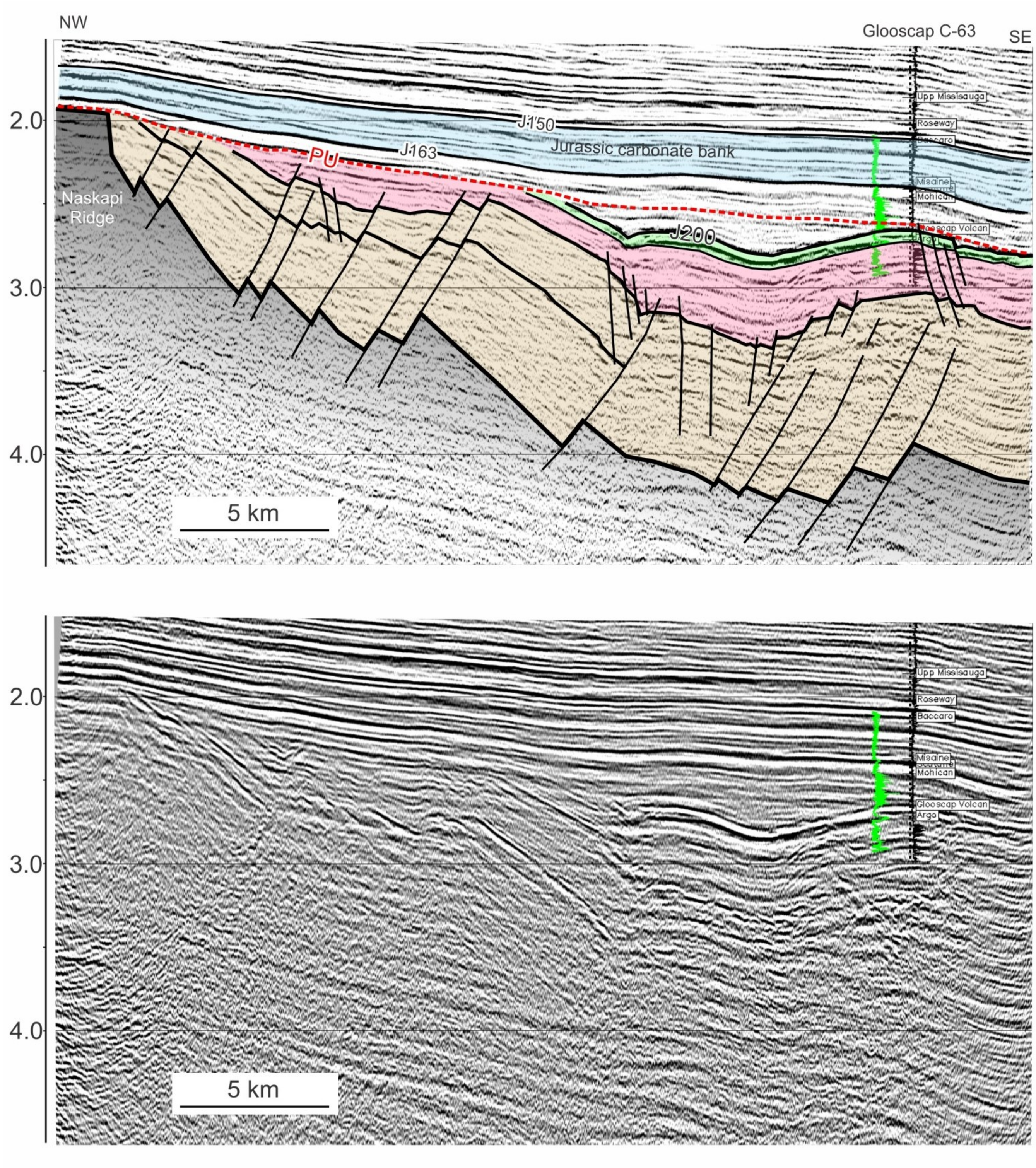

Figure 3.3. Uninterpreted and interpreted profile (Husky HM82-306) across Mohican Graben showing the Glooscap C-63 well tie. Green shading identifies CAMP-related volcanics. Pink shading identifies Late Triassic interval of bedded salt or laterally equivalent continental clastic facies, above heavily faulted older fluvial-lacustrine(?) rift successions (brown shading). Red dashed line corresponds to the postrift unconformity (PU). See Figure 3.1 for line location.

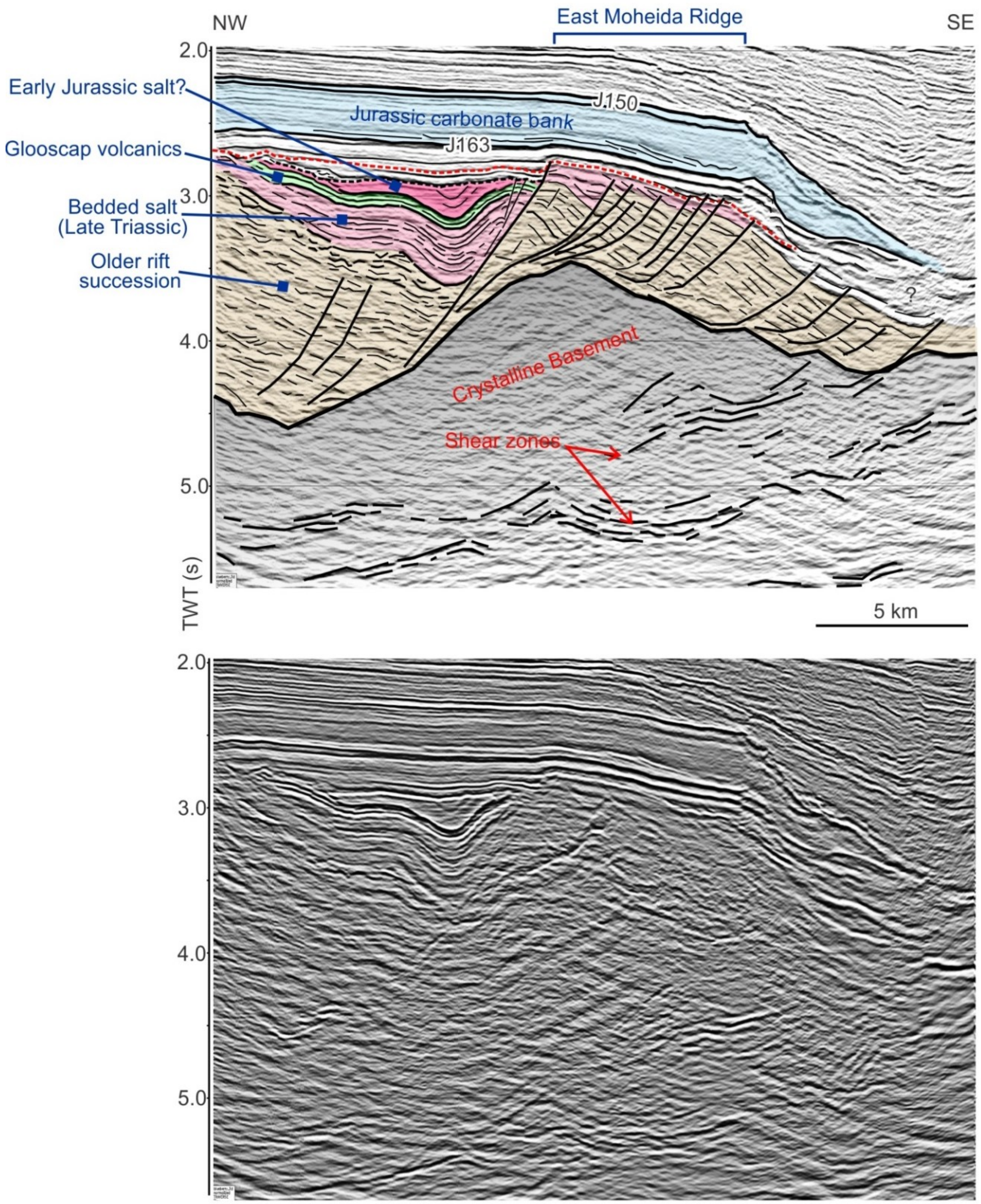

Figure 3.4. Uninterpreted and interpreted profile from the Blueberry 3D survey (CNSOPB program number NS24-E043-004E) across the seaward margin of the Oneida Graben and the East Moheida Ridge. The ridge is comprised of an elevated basement element veneered by a complexly faulted synrift succession. See Figure 3.1 for line location.

basement shows the distribution of Triassic or older rift basins, partly eroded by the postrift unconformity (Figure 3.6a). This early rift succession locally exceeds 1.8 sec (twt) or > 4.4 km thick (using 4.9 km/s velocity for synrift clastics proposed by Wade and MacLean, 1990). The deepest rift deposits (lower part of the brown interval in Figure 3.2) form a tightly faulted succession containing widespread bright amplitude reflections that can be correlated between rift basins. These may correspond to older synrift volcanics or lacustrine facies, but calibration is not available to confirm this. The shallower part of the brown interval (Figure 3.2) is mixed in character, ranging from low amplitude discontinuous to high amplitude continuous reflections, but like the deeper interval, it is generally offset by numerous smaller scale faults.

In the Oneida and Mohican grabens, there is a very abrupt upward change into a layered succession of moderate amplitude continuous reflections capped by the Glooscap volcanics (Figures 3.3, 3.4). The interval drapes or onlaps underlying faulted strata, and is largely unaffected by synsedimentary faults (i.e. faulting in this interval post-dates deposition). This distinct interval appears to be the only part of this Triassic synrift succession (beneath the J200 surface) that has been calibrated in the Mohican Graben. At the base of Glooscap C-63, this layered interval corresponds to a 441 m thick interval of Late Triassic (Rhaetian to late Norian; Weston et al. 2012) bedded salt. The layer is made up of salt interbedded with meter-scale dolomite, red dolomitic shale and siltstone beds, and one 40 m thick red shale to siltstone dominated interval located between 4323 and 4363 m. A similar 55 m thick shale to siltstone dominated interval caps the bedded salt succession between 4046 m and 4101 m. Moheida P-15 encountered a 255 m mixed clastic succession of the Eurydice Formation that, based on seismic correlation, appears to be a laterally equivalent facies of the bedded salt at Glooscap C-63. Mohican I-100 encountered a thin (<100 m) interval of probable Late Triassic shale with the well bottoming a few meters into probable Late Triassic salt (Weston et al. 2012). As such, only the shallowest <450 m of this potentially >4.4 km thick succession has been penetrated in wells, and only in the Mohican Graben. No wells penetrate synrift strata in the Oneida Graben.

A time-structure map on the J200 surface reveals that the Glooscap volcanics and the underlying bedded salt were folded and faulted into long and narrow northeast trending basins adjacent to the Moheida and East Moheida ridges (Figure 3.5a). The J200 surface has a substantial amount of relief (more than 700 ms twt in some places). Much of this relief developed through rejuvenated extension, and inversion, after emplacement of the Glooscap volcanics, consistent with Withjack et al (1998) who suggested rifting continued after CAMP along this part of the Atlantic margin. A time-thickness map between the relatively flat-lying Middle Jurassic J163 marker (top Scatarie Member) and the rugose J200 surface indicates that earliest Jurassic to Callovian strata were preferentially preserved along these long and narrow basins (Figure 3.6b). The basins broaden and deepen to the southwest towards the mouths of the Mohican and Acadia grabens where salt expulsion provided accommodation for late synrift and postrift strata.

There is a noticeable change in the seismic character – from the well layered bedded salt interval at Glooscap C-63 to more incoherent and chaotic seismic facies towards the mouths of the Mohican and Acadia grabens. This is interpreted to reflect a lateral facies change to more massive salt where rift subsidence was greatest. In addition, on some seismic profiles there appears to be a second younger interval of salt above the Glooscap volcanics (i.e. Early Jurassic salt), but further seaward it is not possible to distinguish these two salt intervals. A conspicuous weakly bedded to transparent interval is also present in the Oneida Graben above the folded Glooscap volcanics (Figure 3.4). Acoustically it is quite similar to intervals of autochthonous salt mapped elsewhere on the margin. A final period of extension postdates these deposits, and the remaining relief within the Mohican, Acadia, and Oneida grabens was infilled by Mohican or equivalent Iroquois facies (Figure 1.2; Wade and MacLean, 1990). A more detailed account of the

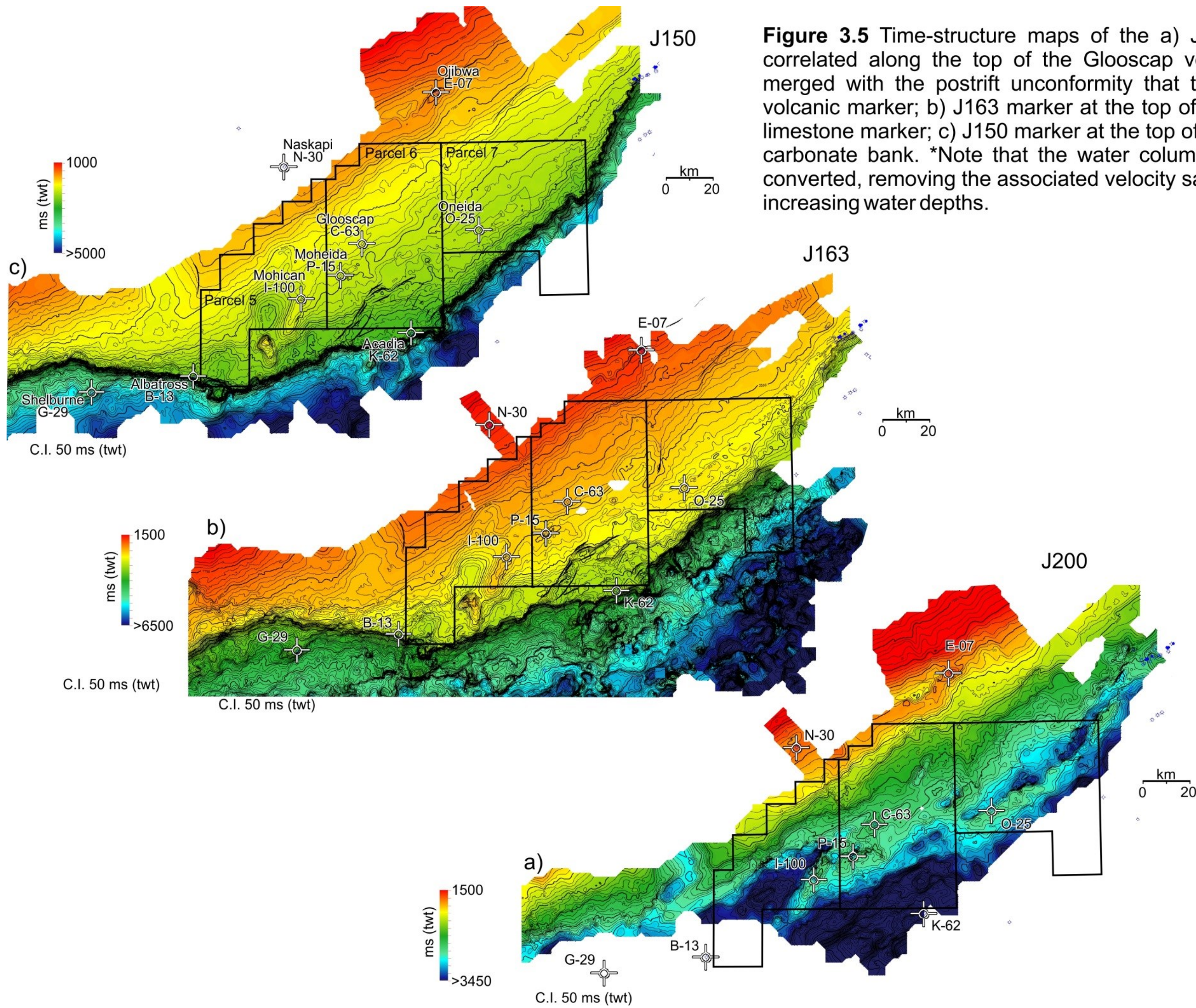

Figure 3.5 Time-structure maps of the a) J200 marker, correlated along the top of the Glooscap volcanics and merged with the postrift unconformity that truncates the volcanic marker; b) J163 marker at the top of the Scatarie limestone marker; c) J150 marker at the top of the Jurassic carbonate bank. *Note that the water column was depth converted, removing the associated velocity sag caused by increasing water depths.

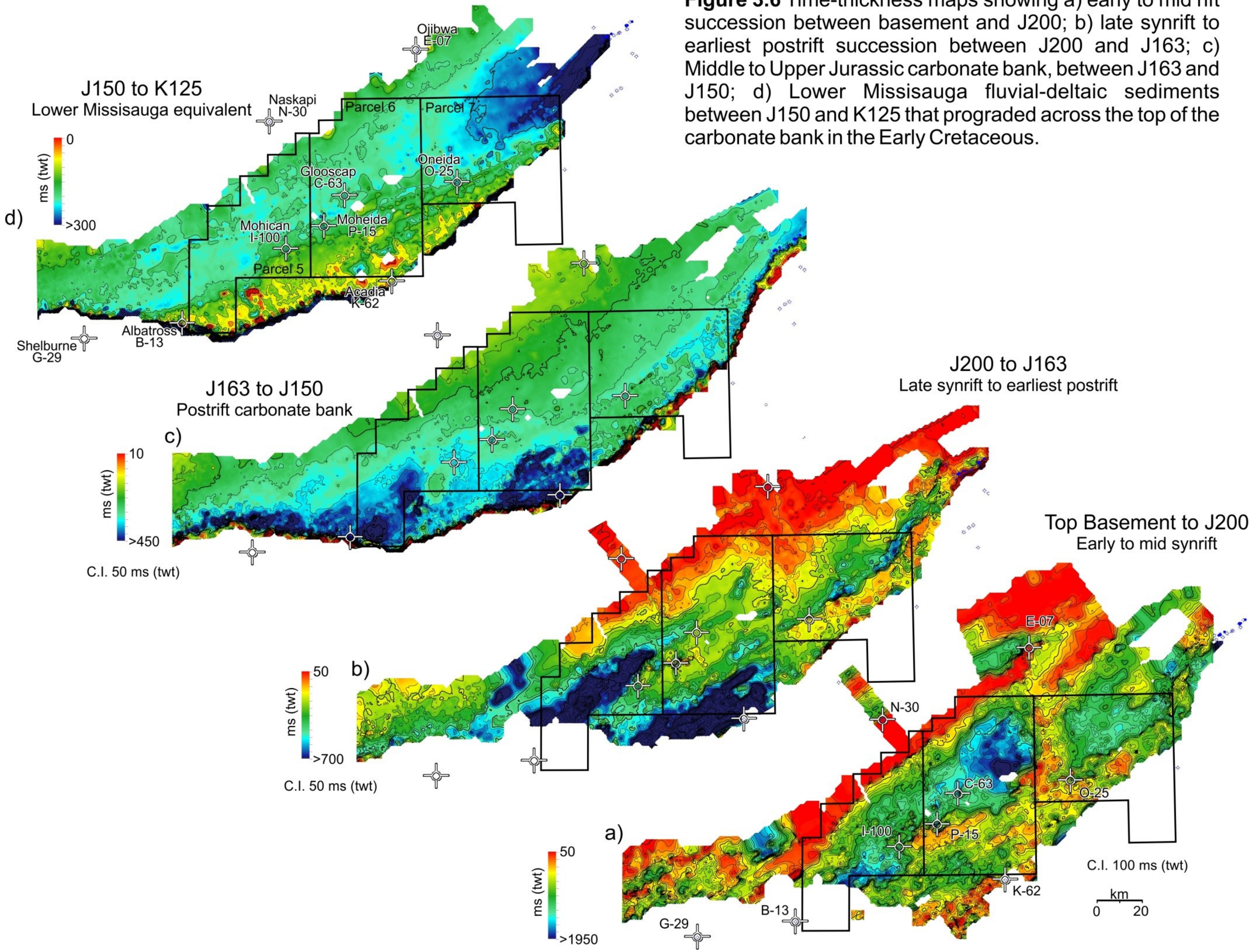

Figure 3.6 Time-thickness maps showing a) early to mid rift succession between basement and J200; b) late synrift to earliest postrift succession between J200 and J163; c) Middle to Upper Jurassic carbonate bank, between J163 and J150; d) Lower Missisauga fluvial-deltaic sediments between J150 and K125 that prograded across the top of the carbonate bank in the Early Cretaceous.

development of these rift basins is currently in progress (Deptuck, in prep).

The overlying Middle to Upper Jurassic carbonate platform developed above the synrift to early postrift deposits described above. Its seaward edge parallels and directly overlies the East Moheida and Acadia ridges, but cuts obliquely across the Moheida and Shelburne ridges. Widespread detachment of younger (mainly Jurassic) postrift cover strata took place in areas where underlying salt was thickest – principally at the mouths of the Mohican and Acadia grabens. Continued expulsion of salt into the Late Jurassic probably accounts for the increased thickness of the carbonate bank above these regions (Figure 3.6c). One large diapir pierces Jurassic and Cretaceous strata southwest of Mohican I-100 (Figure 2.13; Deptuck 2011a). The salt at the mouths of these grabens appears to have welded out (at least on the shelf) by the Early Cretaceous when an influx of clastic sediment from the northeast drowned the carbonate bank (lower part of the Missisauga Formation; Figure 3.6d).

Parcel Descriptions and Exploration Potential

Parcels 5, 6, and 7 are located on the outer shelf and upper slope of the central Scotian margin, extending into 1580, 840, and 2360 m of water, respectively. The parcels border Shell's Exploration Licence 2430 and BP's Exploration Licence 2431. Parcel 5 is located principally above the western part of the Mohican Graben, where widespread detachment of cover strata took place above thicker intervals of synrift salt (as described above). Parcel 6 is located above the eastern part of the Mohican Graben, extending across the Moheida Ridge to the eastern parts of the Acadia Graben (Figure 3.1). Parcel 7 is located mainly above the Oneida Graben, extending across the East Moheida Ridge (Figure 3.1). Both Parcels 5 and 6 are located principally inboard the Jurassic carbonate bank edge, while Parcel 7 extends across the carbonate bank edge and onto the carbonate foreslope (similar to Parcels 3 and 4 in the southwestern region).

Although three wells in the Mohican Graben penetrated the uppermost parts of the synrift succession (Mohican I-100, Moheida P-15, and Glooscap C-63), seismic data indicate that they sample less than 10% of the total rift succession. More broadly, these three wells, combined with Sambro I-29 located 45 km northwest of the Mohican Graben, are the only wells west of the Orpheus Graben (Figure 1.1) to sample synrift strata on the entire Scotian margin. No wells penetrate any of the rift succession in the Oneida or Acadia grabens in Parcels 6 and 7. As such, the hydrocarbon potential of the synrift succession in the Central region, as with elsewhere, is poorly understood and hinges in large part on whether or not synrift lacustrine source rocks could have accumulated in the deeper parts of grabens. Such deposits could have formed during early rift extension when the margin was located at lower paleolatitudes with associated wetter climates more favourable for source rock development (Brown 2014; see also the source rock section below). Kettanah (2011) identified liquid and vaporous hydrocarbons in fluid inclusions within salts of the Late Triassic-Early Jurassic Argo Formation from the Glooscap C-63 and Weymouth A-45 wells. The characteristics of the liquids were determined to be characteristic of "complex, high molecular weight, aromatic or cyclic hydrocarbon compounds higher than methane". The author commented that given their stratigraphic position, the potential source could have been the underlying sediments of the Norian-Rhaetian Eurydice Formation. It is possible that some of the brighter amplitude continuous reflections contained in the lower, heavily faulted rift succession (described earlier) correspond to a fluvial-lacustrine succession containing potential source rocks. The presence of large interconnected lakes during early rifting could explain why these facies can be correlated between rift grabens in the Central region.

If synrift source rocks are present in the Central region, a wide variety of untested synrift targets may exist in Parcels 5, 6, and 7. The Blueberry 3D survey provides excellent imaging of the synrift succession just east of Parcel 7. It shows the development of widespread inversion structures that could form excellent traps, particularly where they are sealed by Late Triassic salt (Figure 3.7a). Similarly, the bedded salt interval encountered at Glooscap C-63 is widespread, draping

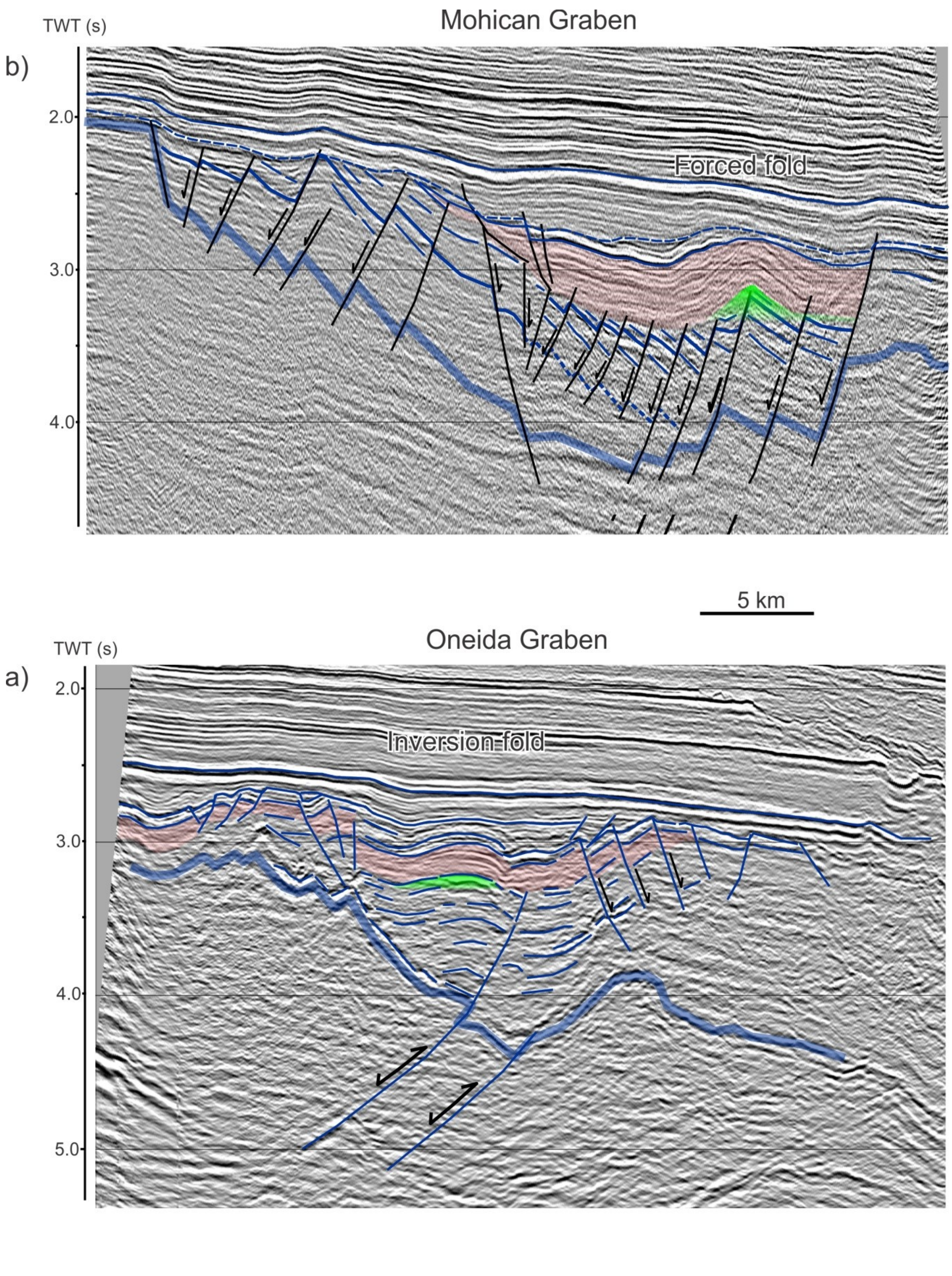

Figure 3.7 Potential pre-salt traps involving synrift fluvial-lacustrine reservoirs draped by bedded salt; a) Synrift reservoirs incorporated into inversion folds and sealed by Late Triassic bedded salt; b) Synrift reservoirs sealed by a forced fold composed of Late Triassic bedded salt.

underlying rotated faults blocks (Figure 3.7b). In some areas, the bedded salts may form a widespread seal above earlier synrift reservoirs. No wells in this region have tested this pre-salt play concept or the deeper synrift strata. Above this rift succession, the Jurassic carbonate bank may also have additional untested potential, particularly in Parcel 7 which crosses the bank edge. Like Parcels 3 and 4, however, new 3D seismic data-sets will be needed to identify new targets in the Jurassic carbonate bank, as with the underlying complex Triassic rift succession.

Acknowledgements – We wish to thank Kris Kendell, Brent Smith, Shaun Rhyno, and Carl Makrides of the CNSOPB, and Francky Saint-Ange, Dimitri Savva, and Tomasz Chrest of Beicip-Franlab for helpful discussions. We also thank Janice Weston, Andrew MacRae, Rob Fensome and the rest of the biostratigraphic team for their continued efforts to refine age calibration in the Nova Scotia offshore area.

References

Austin, J.A., Uchupi, E., Shaughnessy, D.R., and Ballard, R.D. (1980), Geology of New England passive margin, AAPG Bulletin, v. 64, p. 501-526

Brown, D.E. (2014) Lacustrine source rock potential in the Middle Triassic – Early Jurassic Chignecto Subbasin, offshore Eastern Canada. Geological Association of Canada/ Mineralogical Association of Canada Annual Meeting, University of New Brunswick, Fredericton, New Brunswick, May 21-23, 2014.

Campbell, D.C. (2011) The Late Cretaceous and Cenozoic geological history of the outer continental margin off Nova Scotia, Canada: Insights into margin evolution from a mature passive margin, PhD Dissertation, Department of Earth Sciences, Dalhousie University, Halifax, Nova Scotia, 286 p.

Campbell, D.C. and Deptuck, M.E. (2012) Alternating bottom current dominated and gravity flow dominated deposition in a lower slope and rise setting – insights from the seismic geomorphology of the western Scotian margin, Eastern Canada, In: B. Prather, M. Deptuck, D. Mohrig, B. van Hoorn, and R. Wynn (Eds), Application of the Principles of Seismic Geomorphology to Continental Slope and Base-of-slope Systems: Case Studies from Seafloor and Near-Seafloor Analogues, SEPM Special Publication 99, p. 329-346

Deptuck, M.E. (2010) The 'slope detachment zone' on the western Scotian Slope, offshore Nova Scotia: structural style, timing, and implications for margin evolution, In: Conjugate Margins II, Lisbon 2010, Metedo Directo, v. IV, p. 87-95, ISBN: 978-989-96923-1-2, http://metedodirecto.pt/CM2010 www.cnsopb.ns.ca

Deptuck, M.E. (2011a) Proximal to distal postrift structural provinces on the western Scotian Margin, offshore Eastern Canada: Geological context and parcel prospectivity for Call-for-Bids NS11-1, Canada-Nova Scotia Offshore Petroleum Board, Geoscience Open File Report (GOFR) 2011-001MF, 42p. www.cnsopb.ns.ca/sites/default/files/pdfs/

Deptuck, M.E. (2011b) Potential shelf sources for deepwater reservoirs along the southwestern Scotian margin, and the impact of a hybrid 'bypass-ponded' slope on reservoir distribution, AAPG Seminar, http://energy.novascotia.ca/oil-and-gas/offshore/play-fairway-analysis/data-and-presentations (accessed Nov 2012)

Deptuck, M.E. and Campbell, D.C. (2012) Widespread erosion and mass failure from the ~51 Ma Montagnais marine bolide impact off southwestern Nova Scotia, Canada, Canadian Journal of Earth Sciences, v. 49, p. 1567-1594

Deptuck, M.E., Kendell, K., Brown, D., Smith, B. (2014) Seismic stratigraphic framework and structural evolution of the eastern Scotian Slope: geological context for the NS14-1 Call for Bids area, offshore Nova Scotia, CNSOPB Geoscience Open File Report 2014-001MF, 58 p

Dehler, S.A. and Roest, W.R. (1998) Gravity anomaly map, Atlantic Region, Canada. Geological Survey of Canada Open File 3658, Scale 1:3,000,000

Dore, G. and Robbins, J. (2005) The buzzard Field, In: A.G. Dore and B.A Vinning (Eds) Petroleum Geology: North-West Europe and Global Perspectives – Proceedings of the 6th Petroleum Geology Conference, p. 241-252

Elliott, E.T. and Post, P.J. (2012) Atlantic Well Folio: Georges Bank Basin, Lydonia Canyon Block 133 No. 1 Well, BOEM 2012-089

Given, M.M. (1977) Mesozoic and Early Cenozoic geology of offshore Nova Scotia, Bulletin of Canadian Petroleum Geology, v. 25, p. 63-91

Grow, J.A., Hutchison, D.R., Klitgord, K.D., Dillion, W.P., and Schlee, J.S. (1983) Representative multichannel seismic profiles over the U.S. Atlantic margin, In: A.W. Bally (Ed) Seismic expression of structural styles, AAPG Studies in Geology 15, p. 2.2.3-1 to 2.2.3-18

Hurtubise, D.O., Puffer, J.H., and Cousiminer, H.L. (1987) An offshore Mesozoic igneous sequence, Georges Bank basin, North Atlantic, Geological Society of America Bulletin, v. 98, p. 430-438

Hutchison, D.R. and Klitgord, K.D. (1988) Evolution of rift basins on the continental margin off southern New England, In: W. Manspeizer (Ed) Triassic-Jurassic Rifting: Continental Breakup and the Origin of the Atlantic Ocean and Passive Margins, Part A, Elsevier, p. 81-98

Jackson, M.P.A., Cramez, C., and Fonck, J-M. (2000) Role of subaerial volcanic rocks and mantle plumes in creation of South Atlantic margins: implications for salt tectonics and source rocks, Marine and Petroleum Geology, v. 17, p. 477-498

Keen, C.E., and Potter, D.P. (1995) Formation and evolution of the Nova Scotia rifted margin: Evidence from deep seismic reflection data, Tectonics, v. 14, p. 918-932

Keen, C.E., Loncarevic, B.D., Reid, I., Woodside, J., Haworth, R.T., and Williams, H. (1990) Tectonic and geophysical overview, Chapter 2, In: M.J. Keen and G.L. Williams, (Eds) Geology of the Continental Margin of Eastern Canada, , Geological Survey of Canada, The Geology of Canada, p. 33-85

Kendell, K. (2012) Variations in salt expulsion style within the Sable Canopy Complex, central Scotian margin, Canadian Journal of Earth Sciences, v. 49, p. 1504-1522

Kidston, A.G., Brown, D.E., Smith, B.M., and Altheim, B. (2005) The Upper Jurassic Abenaki Formation, offshore Nova Scotia: A seismic and geologic perspective, Canada Nova Scotia Offshore Petroleum Board, Halifax, Nova Scotia, 168 p. www.cnsopb.ns.ca

Kidston, A.G., Smith, B.M., Brown, D.E., Makrides, C., and Altheim, B. (2007) Nova Scotia deepwater post-drill analysis, 1982-2004, Canada Nova Scotia Offshore Petroleum Board, Halifax, Nova Scotia, 181 p. www.cnsopb.ns.ca

Kontak, D.J. and Archibald, D.A. (2003) $^{40}Ar/^{39}Ar$ age of the Jurassic North Mountain Basalt, southwestern Nova Scotia, Atlantic Geology, v. 39, p. 47-53

Larsen, H.C., Saunders, A.D., Clift, P.D. et al. (1994) Proceedings of the Ocean Drilling Program, Initial Reports, v. 152

MacDonald, A. (2011). Play Fairway Analysis – Shelburne Delta, AAPG Seminar, available at: http://energy.novascotia.ca/oil-and-gas/offshore/play-fairway-analysis/data-and-presentations (accessed Nov 2012)

Magee, C. Hunt-Stewart, E., Jackson, C.A.-L. (2013) Volcano growth mechanism and the role of sub-volcanic intrusion: Insights from 2D seismic reflection data, Earth and Planetary Science Letters, v. 373, p. 41-53

Manspeizer, W. (1988) Triassic-Jurassic rifting and opening of the Atlantic: An overview, In: W. Manspeizer (Ed) Triassic-Jurassic Rifting: Continental Breakup and the Origin of the Atlantic Ocean and Passive Margins, Part A, Elsevier, p. 42-79

McAlpine, K.D. (1990) Mesozoic stratigraphy, sedimentary evolution and petroleum potential of the Jean d'Arc basin, Grand Banks of Newfoundland, Geological Survey of Canada Paper 89-17, 50p.

Oakey, G.N., and Dehler, S.A. (2004) Magnetic anomaly map, Atlantic Canada region, Atlantic Canada. Geological Survey of Canada Open File 1813, Scale 1:3,000,000

OETR (2011) Play Fairway Analysis Atlas - Offshore Nova Scotia, Nova Scotia Department of Energy Report, NSDOE Records Storage File No. 88-11-0004-01, 347p. http://www.offshoreenergyresearch.ca/OETR/OETRPlayFairwayProgramMainPage/tabid/402/Default.aspx

Pe-Piper, G., Jansa, L.F. and Lambert, R. St. J. (1992), Early Mesozoic magmatism on the Eastern Canadian Margin: Petrogenetic and tectonic significance. In: J.H. Puffer and P. Ragland (Eds) *Mesozoic Magmatism of Eastern North America*, Special Publication of the Geological Society of America Special Publication 268, p.13-36.

Pe-Piper, G. and Jansa, L.F. (1999) Pre-Mesozoic basement rocks offshore Nova Scotia, Canada: new constraints on the origin and Paleozoic accretionary history of the Meguma terrane, Bulletin of the Geological Society of America, v. 111, p. 1773-1791

Pe-Piper, G. and Piper, D.J.W. (2004) The effects of strike-slip motion along the Cobequid-Chedabucto-southwest Grand Banks fault system on the Cretaceous-Tertiary evolution of Atlantic Canada, Canadian Journal of Earth Sciences, v. 41, p. 799-808

Poag, C.W. (1991) Rise and demise of the Bahama-Grand Banks gigaplatform, northern margin of the Jurassic proto-Atlantic seaway, Marine Geology, v. 102, p. 63-130

Poppe, L.J. and Poag, C.W. (1993) Mesozoic stratigraphy and paleoenvironments of the Georges Bank Basin: A correlation of exploratory and cost wells, Marine Geology, v. 113, p. 147-162

Schlee, J.S. and Klitgord, K.D. (1988) Georges Bank Basin: A regional synthesis, In: R.E. Sheridan and J.A. Grow (Eds) The Geology of North America, Volume I-2, The Atlantic Continental Margin, U.S. Geological Society of America, p. 243-268

Shimeld, J. (2004) A comparison of salt tectonic subprovinces beneath the Scotian Slope and Laurentian Fan. In: P.J. Post, D.L. Olsen, K.T. Lyons, S.L. Palmes, P.F. Harrison, and N.C. Rosen (Eds) Salt-Sediment Interactions and Hydrocarbon Prospectivity: Concepts, Applications, and Case Studies for the 21st Century, 24th Annual GCS-SEPM Foundation Bob F. Perkins Research Conference, Houston, p.502-532, CD-ROM.

Wade, J.A. and MacLean, B.C. (1990) The geology of the Southeastern Margin of Canada, Chapter 5, In: M.J. Keen and G.L. Williams (Eds), Geology of the Continental Margin of Eastern Canada, Geological Survey of Canada, The Geology of Canada, p. 224-225

Welsink., H.J., Dwyer, J.D. and Knight, R.J. (1989) Tectono-stratigraphy of the passive margin off Nova Scotia, Chapter 14, In: A.J. Tankard and H.R. Balkwill (Eds) Extensional Tectonics and Stratigraphy of the North Atlantic Margins, AAPG Memoir 46, p. 215-231.

Weston, J.F., MacRae, R.A., Ascoli, P., Cooper, M.K.E., Fensome, R.A., Shaw, D. and Williams, G.L. (2012) A revised biostratigraphic and well-log sequence stratigraphic framework for the Scotian Margin, offshore eastern Canada, Canadian Journal of Earth Sciences, v. 49, p. 1417-1462

Withjack, M.O., Schlische, R.W., and Olsen, P.E. (1998) Diachronous rifting, drifting and inversion on the passive margin of central Eastern North America: An analogue for other passive margins, AAPG Bulletin, v. 82, p. 817-835